Department of Mechanical Engineering
Solid Mechanics

ISRN LUTFD2/TFHF-06/5122-SE(1-80)

DROP TEST OF A SOFT BEVERAGE PACKAGE – EXPERIMENTAL TESTS AND A PARAMETER STUDY IN ABAQUS

Master's Dissertation by

Johanna Lönn
and
Jenny Navréd

Supervisors

Eskil Andreasson, Tetra Pak R&D AB, Sweden
Håkan Hallberg, Div. of Solid Mechanics, Lund University, Sweden
Magnus Harrysson, Div. of Solid Mechanics, Lund University, Sweden

Printed by Media-Tryck, Lund University, Lund, Sweden
For information, adress:
Division of Solid Mechanics, Lund University, Box 118, SE-221 00 Lund, Sweden
Homepage: http://www.solid.lth.se

Acknowledgement

The research presented in this master's thesis was carried out at Tetra Pak R&D AB in Lund in cooperation with the Division of Solid Mechanics at the University of Lund, Sweden, during October 2005 to March 2006.

At first we would like to express our deepest gratitude to our supervisor M.Sc Eskil Andreasson at Tetra Pak R&D AB, for his support and guidance throughout this project. Without his assistance and devotion this thesis would have been difficult to complete.

Further a great thanks to our supervisors PhD students Magnus Harrysson and Håkan Hallberg at the Division of Solid Mechanics, for their help with the theory and helpful ideas.

We would also like to thank the staff at Tetra Pak in Lund for valuable input to the project and their help.

Lund, April 2006

Johanna Lönn and Jenny Navréd

Abstract

Beverage packages are tested in many ways at Tetra Pak to determine their properties. In this master's thesis the drop test method will be considered. The goal is to evaluate the possibilities to perform FE-simulations of the dynamic drop test procedure. A wish is to establish a parameter that will predict if the package can resist an impact from a desired height.

The FE-simulations will be performed in the computer software ABAQUS/ Explicit since this program is suitable for dynamic impact problems. Three various modelling techniques have been tried out and a skin modelling method was selected. This method is easy to use and the best interaction between the liquid product and the package was received. The FE-model in the simulation is simplified to obtain a model that is easy to handle. Simplifications have been made on the transversal sealing and no initial folds have been introduced. The packaging material contains paperboard and thereby the laminate structure has orthotropic properties in the elastic and plastic area which will be assigned in the FE-model. The fluid properties are assigned by an equation of state, EOS, to represent the fluid behaviour in ABAQUS/Explicit.

It has been detected that the failure in the package during a drop test often occurs in the area of the transversal sealing. The test method that will be considered to evaluate the strength in the transversal sealings is the dynamic pendulum. Unfortunately no satisfying result was obtain from the pendulum setup used in this thesis and therefore the transversal sealings cannot be evaluated.

The main purpose with this thesis is accomplished since it is possible to FE-simulate a drop test procedure of a soft beverage package. The results that are captured in the simulations are evaluated against each other and high-speed films. The behaviour in the FE-simulations are similar between the simulated drop heights. The high-speed films indicate on the same be-

haviour as the FE-simulations show. An interesting discovery is that shear stress concentrations are usually located in the same areas that cracks appear in the packaging material. The MD stresses increase with the drop height. This corresponds well to reality since more packages are damaged when dropped from higher heights. It is also established that the orientation of the package in a drop test highly affect the result of the test. This is determined by examine the reaction forces during impact in the FE-simulations.

Keywords: drop-test, FE-simulation, ABAQUS/Explicit, hardening models, beverage packages.

Contents

Chapter 1

Introduction

Tetra Pak is one of the big companies on the liquid carton based packaging market. All around the world beverages are packed in Tetra Pak packages. The product that will be studied in this master's thesis is a soft aseptic pouch. The challenge is to develop a package with acceptable properties even though the packaging material is relatively thin.

1.1 Background

Beverage packages are tested in many ways to determine their properties. One way is to perform drop tests that give an approximated value of the drop height for the package. This method has to be performed at a large number of packages to evaluate the ability of the packages to resist an impact. An interesting idea is to investigate whether it is possible to perform Finite Element simulations, FE-simulations, of the drop test procedure. This would bring benefits to the development time which could be reduced since the FE-simulation can provide essential information in the choice of packaging material. A wish at Tetra Pak R&D regarding this thesis is to be able to predict a drop height that will not result in damaged packages.

1.2 Problem formulation

The main problem in this thesis is to investigate whether it is possible to FE-simulate with a finite element model, FE-model, a soft package containing a liquid product during impact. The FE-simulations will be performed in the computer program ABAQUS/Explicit. The difficulties are to solve the large deformations due to the fluid and material properties. If this problem is solved the next step will be to investigate whether there is a parameter to

evaluate and compare against to detect differences in packaging materials. This evaluation will be done in both FE-simulations and experimental tests.

1.3 Objectives

The primary goal of this thesis is to investigate the possibility to FE-simulate the soft package during impact. The following goals are defined if the primary goal is achieved. One of these goals is to determine a parameter that can be used to predict the critical drop height of a packaging material. Another goal is to evaluate the FE-simulation possibilities with this type of model.

1.4 Limitations and assumptions

The FE-simulation model will be simplified since the geometry and sealings are complex. All folds and imperfections are eliminated in order to simplify the modelling procedure. The packaging material will be considered as one material and not as a laminate structure. This limitation will shorten the solution time. The milk product is simplified to water since the differences are assumed to be negligible.

Chapter 2

Package information

The shape of the package used in this thesis is the same as the already existing TFA pouch, Tetra Fino Aseptic. The volume of the package is 250 ml. The manufacturing process of the package is simple and contains only a few steps. The package material is fed from a roll of material, according to Figure 2.1, and then the material is sterilized and finally formed to a tube. The tube is filled with product and sealed in both ends. The idea of an aseptic package is that it can be kept at room temperature without spoiling the product.

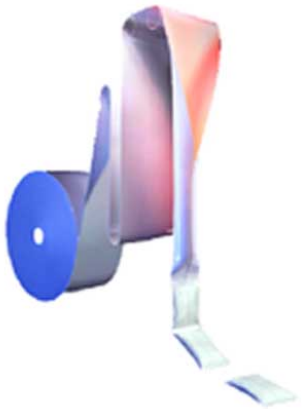

Figure 2.1: Manufacturing process of an aseptic pounch [1].

2.1 The packaging material

The packaging material contains polymer and paperboard layers. To protect the milk a polymer layer is used as a light barrier. When using paperboard as packaging material it is important to be aware of the orthotropic properties.

Orthotropic behaviour means that the material has different properties in the three directions according to Figure 2.2. The reason paperboard has orthotropic behaviour is due to that the fibers are oriented in the paperboard manufacturing process. Primarily the fibers are oriented in the plane where the machine direction, MD, is the dominating one. The other directions are the cross machine direction, CD, and the out of plane direction, ZD.

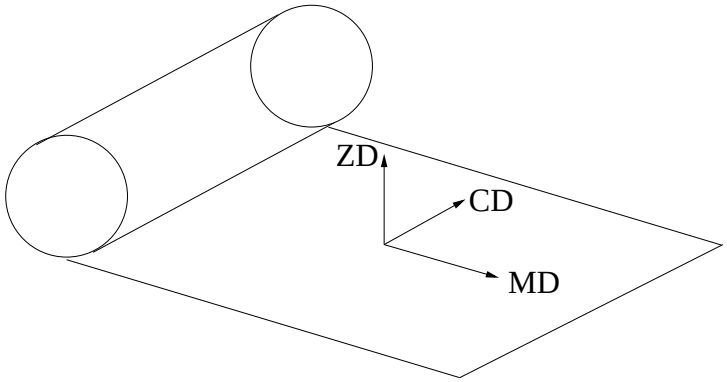

Figure 2.2: Paperboard properties in different direction.

2.2 The packaging sealings

There are different types of sealing techniques that are used in different types of machine systems and materials, to achieve a desirable strength in the sealings. The package has two types of sealings, longitudinal and transversal, as presented in Figure 2.3. The longitudinal sealing is created by an overlap along the sides when forming the tube in the filling process. To prevent penetration of liquid in the packaging material a polymer strip is placed over the longitudinal sealing. In the package impulse heating is used for the transversal sealings. During the sealing process the tube is sealed and cut into packages. Two jaws squeeze the tube together in intervals. In a squeeze motion the jaw seals the top of the lower package and the bottom in the package above the lower package as shown in Figure 2.1.

2.3 The product in the package

The product in the package is as mentioned milk. To be more precise it is UHT, ultra heat treated, milk which means that the milk can be stored at room temperature in a sterile package. The content in the package is water

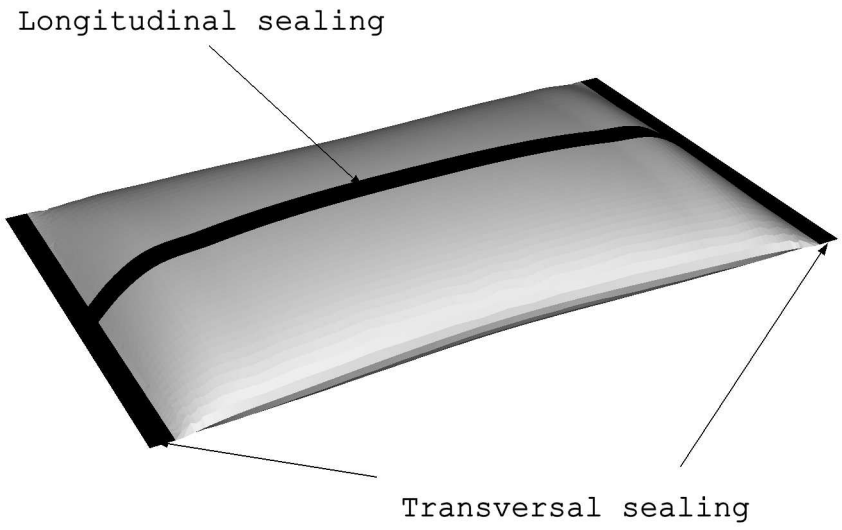

Figure 2.3: Longitudinal and transversal sealings in the package.

during the development process since milk is too expensive. The differences between milk and water are assumed to be negligible in this thesis since the drop tests are performed with water.

Chapter 3

Theory

This chapter will cover the theory used in this thesis. The theory is needed in order to understand the deformation aspects and the choice of material model. The theory that is described in this chapter is used in the computational solution program. The main topics that will be described are continuum mechanics, equation of motion and constitutive models.

3.1 Continuum mechanics

This section covers the essential parts of continuum mechanics. At first the basic theory of large deformation is introduced followed by strain and stress measures. The equation of motion will then be reformulated to the principle of virtual power.

3.1.1 Kinematics of large deformations

Consider a body Ω_0 as shown in Figure 3.1 at the initial time $t = 0$. This state is called the initial or reference configuration. After displacement or deformation the body has a new position, denoted Ω. This is the deformed configuration. The vector X_j is given from the origin to a material point in the reference configuration. The vector x_i is described in the same way for the deformed configuration. The displacement vector u_i is the difference between two material points [2]. The motion from the reference to the deformed configuration is described by

$$x_i = x_i(X_j, t) \tag{3.1}$$

Consider two material points close to each other in the same configuration. The line segment between these points is denoted dX_j in the reference con-

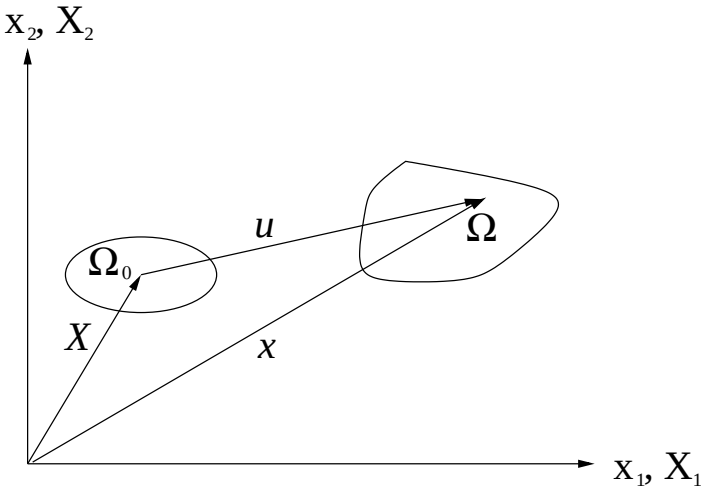

Figure 3.1: Deformation from initial to deformed configuration [2].

figuration respectively dx_i in the deformed configuration. The linear relation between the line segments is uniquely defined by

$$dx_i = F_{ij} dX_j \tag{3.2}$$

where F_{ij} is the deformation gradient tensor which is defined as

$$F_{ij} = \frac{\partial x_i}{\partial X_j} \tag{3.3}$$

and

$$det(F_{ij}) > 0 \tag{3.4}$$

The polar decomposition theorem states that in continuum mechanics a deformation gradient tensor F_{ij} can be decomposed into a rotation matrix R_{ik} and a left stretch tensor V_{kj} [2].

$$F_{ij} = R_{ik} V_{kj} \tag{3.5}$$

3.1.2 Strain measures

The strain measure that will be considered in this thesis is the logarithmic strain [3].

$$\varepsilon_{kj} = ln(V_{kj}) \tag{3.6}$$

This strain measure is appropriate for large deformation analysis since the elastic part is assumed to be small [3]. To define the rate of deformation in the system the velocity of a material particle is defined as

$$v_i = \frac{\partial x_i}{\partial t} \tag{3.7}$$

The velocity difference between two neighboring particles in the deformed configuration is

$$dv_i = \frac{\partial v_i}{\partial x_j} dx_j = L_{ij} dx_j \tag{3.8}$$

where

$$L_{ij} = \frac{\partial v_i}{\partial x_j} \tag{3.9}$$

is the velocity gradient tensor in the deformed configuration. The velocity gradient tensor L_{ij} can be decomposed into symmetric and antisymmetric parts according to

$$L_{ij} = D_{ij} + W_{ij} \tag{3.10}$$

The rate of deformation tensor D_{ij} is defined by

$$D_{ij} = \frac{1}{2}\left(\frac{\partial v_i}{\partial x_j} + \frac{\partial v_j}{\partial x_i}\right) \tag{3.11}$$

and the spin tensor W_{ij} as

$$W_{ij} = \frac{1}{2}\left(\frac{\partial v_i}{\partial x_j} - \frac{\partial v_j}{\partial x_i}\right) \tag{3.12}$$

3.1.3 Stress measures

The Cauchy stress is based on the deformed configuration and thereby defines the true stresses [2]. The Cauchy stress σ_{ij} is defined as

$$t_i = \sigma_{ij} n_j \tag{3.13}$$

where t_i is the traction vector and n_j is the normal out of the surface in the deformed configuration. Another type of stress measure to consider is the stresses in the reference configuration. These stresses are then calculated on the undeformed surface and are called the nominal stresses, P_{ij}, these are defined in a similar way as the Cauchy stresses. The nominal stresses are used in experimental measures.

$$t_i^0 = P_{ij} n_j^0 \tag{3.14}$$

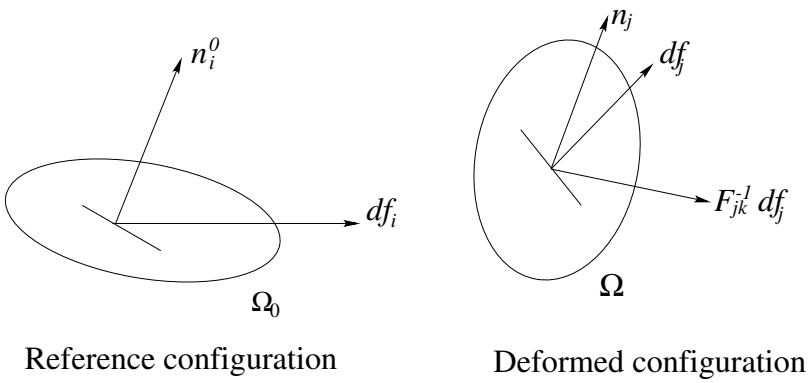

Figure 3.2: Stress measures in current and deformed configuration [2].

3.2 Equation of motion

The equation of motion is formulated for an arbitrary part of the body in the deformed configuration Ω according to Figure 3.2. The arbitrary body has the volume V and a boundary surface S. The arbitrary body is affected by the traction vector along the boundary surface and the inner body force b_i per unit mass in the body [4]. This is adopted in Newton's second law

$$\int_S t_i dS + \int_V \rho b_i dV = \int_V \rho \ddot{u}_i dV \tag{3.15}$$

where ρ is the mass density and $\ddot{u}_i$ is the acceleration. Further the divergence theorem of Gauss states the following relation for an arbitrary vector q_i

$$\int_V \mathrm{div} q_i dV = \int_S q_i n_i dS \tag{3.16}$$

The definition of the divergence of the vector $q_{i,i}$ is

$$\mathrm{div} q_{i,i} = \frac{\partial q_i}{\partial x_i} \tag{3.17}$$

This allows (3.15) to be expressed as

$$\int_V (\sigma_{ij,j} + \rho b_i - \rho \ddot{u}_i) dV = 0 \tag{3.18}$$

where $\sigma_{ij,j}$ is the divergence of the Cauchy stress. Since (3.18) holds for arbitrary regions V of the body, the equation of motion is obtained

$$\sigma_{ij,j} + \rho b_i = \rho \ddot{u}_i \tag{3.19}$$

The equation of motion is called the strong form. The principle of virtual power, also called the weak formulation, is then obtained by multiplying the

strong form with the weight vector, w_i, and integrate over the volume as follows

$$\int_V w_i(\sigma_{ij,j} + \rho b_i - \rho \ddot{u}_i)dV = 0 \tag{3.20}$$

This equation can be written as

$$\int_V [(\sigma_{ij} w_i)_{,j} - \sigma_{ij} w_{i,j}]dV + \int (w_i \rho b_i - \rho w_i \ddot{u}_i)dV = 0 \tag{3.21}$$

Further (3.16) and (3.13) brings that

$$\int_V (\sigma_{ij} w_i)_{,j} dV = \int_S \sigma_{ij} w_i n_j dS = \int_S w_i t_i dS \tag{3.22}$$

The result of (3.22) inserted in (3.21) is

$$\int_V \rho w_i \ddot{u}_i dV + \int_V w_{i,j} \sigma_{ij} dV = \int_S w_i t_i dS + \int_V w_i \rho b_i dV \tag{3.23}$$

This is the weak formulation or the principle of virtual power. The arbitrary vector will be evaluated. The displacement in the deformed configuration may be expressed as

$$x_i = X_i + u_i \tag{3.24}$$

The virtual rate of the displacement will then be expressed as

$$\dot{u}_i^v = \dot{x}_i^v \tag{3.25}$$

The arbitrary vector w_i is now chosen as $\dot{u}_i^v$ and with this choice it follows that

$$\frac{\partial w_i}{\partial x_j} = \frac{\partial}{\partial x_j}\left(\frac{dx_i^v}{dt}\right) = \frac{d}{dt}\left(\frac{\partial x_i^v}{x_j}\right) = L_{ij}^v \tag{3.26}$$

In this expression the rate of deformation L_{ij}^v is related to the arbitrary vector w_i and since the weight function is arbitrary the weak formulation of equation of motion can be formulated as

$$\int_V \rho w_i \ddot{u}_i dV + \int_V D_{ij}^v \sigma_{ij} dV = \int_S w_i t_i dS + \int_V w_i \rho b_i dV \tag{3.27}$$

The deformation gradient $D_{ij}^v = L_{ij}^v$ since σ_{ij} is symmetric. This formulation holds for every material since no constitutive assumptions have been made.

3.3 Constitutive model

To establish the constitutive model the stress rate, the yield stress criterion and the hardening model have to be determined. The formulation of Hill's orthotropic yield criterion will be considered together with three different hardening models. The hardening models that are considered are isotropic, linear kinematic and combined hardening. These models can all be defined in ABAQUS.
At first small deformation is considered

$$\varepsilon_{ij} = \varepsilon^e_{ij} + \varepsilon^p_{ij} \tag{3.28}$$

where ε^e_{ij} is the elastic and ε^p_{ij} is the plastic strains. To establish a similar relation in large deformation theory the deformation rate D_{ij} is considered. The rate of deformation is decomposed into an elastic D^e_{ij} and a plastic D^p_{ij} part as

$$D_{ij} = D^e_{ij} + D^p_{ij} \tag{3.29}$$

An assumption is made that the stress rate is linearly related to the rate of deformation, this is the hypo elastic law.

$$\frac{D\sigma_{ij}}{Dt} = C_{ijkl} D^e_{kl} \tag{3.30}$$

where C_{ijkl} is a constitutive tensor and D^e_{kl} is elastic rate of the deformation tensor from above. This assumption does not account for rigid body motion and therefore (3.30) is modified and called the Green-Naghdi rate

$$\sigma^{GN}_{ij} = C_{ijkl} D^e_{kl} - \dot{R}_{lk} R_{li} \sigma_{kj} - \sigma_{ik} R_{kl} \dot{R}_{jl} \tag{3.31}$$

where R_{ik} is the rotation tensor and $\dot{R}_{lk}$ is the rate of the rotation tensor [2].

3.3.1 Hill's orthotropic yield criterion

The yield criteria defines when a material will enter the plastic region. For an isotropic material the von Mises yield criteria is often used. The yield surface has the shape of a circle in the deviatoric coordinate system according to Figure 3.3 since the stresses are equal in all directions. Materials that behave differently when loaded in different directions are called anisotropic. If a material has three orthogonal symmetry planes the material is then called orthotropic. This means that the material is not fully anisotropic,

examples of orthotropic materials are paper and wood. A way to introduce an orthotropic yield surface is to use the Hill yield criterion

$$F(s_2-s_3)^2+G(s_2-s_1)^2+H(s_3-s_1)^2+2Ls_{23}^2+2Ms_{12}^2+2Ns_{13}^2-1=0 \quad (3.32)$$

The yield surface with the Hill criterion can be seen in Figure 3.3. This criterion is applied to the packaging material that has different properties in the MD and CD. In (3.32) the 1-, 2- and 3-directions correspond to the MD, CD and ZD. The initial yielding in the Hill criterion is assumed to be affected only by deviatoric stresses, s_{ij} [5]. The deviatoric stress is defined as

$$s_{ij} = \sigma_{ij} - \frac{1}{3}\sigma_{kk}\delta_{ij} \quad (3.33)$$

The criterion contains six independent material parameters. These can be determined by uniaxial stress tests and shear tests [6]. The material constants can then be determined as

$$\begin{aligned} F &= \frac{1}{2}\left[\frac{1}{(\sigma_{y0}^1)^2}+\frac{1}{(\sigma_{y0}^3)^2}-\frac{1}{(\sigma_{y0}^2)^2}\right] \\ G &= \frac{1}{2}\left[\frac{1}{(\sigma_{y0}^1)^2}+\frac{1}{(\sigma_{y0}^2)^2}-\frac{1}{(\sigma_{y0}^3)^2}\right] \\ H &= \frac{1}{2}\left[\frac{1}{(\sigma_{y0}^3)^2}+\frac{1}{(\sigma_{y0}^2)^2}-\frac{1}{(\sigma_{y0}^1)^2}\right] \\ L &= \frac{1}{2\left(\sigma_{y0}^{13}\right)^2} \\ M &= \frac{1}{2\left(\sigma_{y0}^{12}\right)^2} \\ N &= \frac{1}{2\left(\sigma_{y0}^{23}\right)^2} \end{aligned} \quad (3.34)$$

where the σ_{y0} is the yield stress. The Hill criterion can only be used when the yield surface is closed. This means that the following relation must be satisfied.

$$\frac{4}{(\sigma_{y0}^1)^2(\sigma_{y0}^3)^2} > \left[\frac{1}{(\sigma_{y0}^2)^2}-\frac{1}{(\sigma_{y0}^3)^2}+\frac{1}{(\sigma_{y0}^1)^2}\right]^2 \quad (3.35)$$

3.3.2 Hardening models

Hardening occurs when the stress in a material passes the yield stress and can be determined by different hardening laws. The initial yield surface is defined as

$$F(\sigma_{ij}) = 0 \quad (3.36)$$

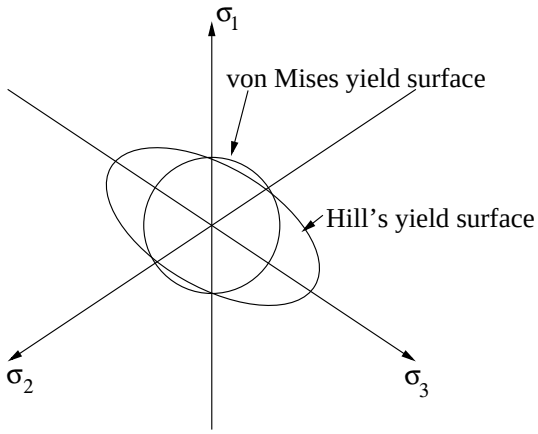

Figure 3.3: Initial yield curve for Hill's and von Mises criterion [5].

and depends only on the stress tensor σ_{ij}. When the plastic strains increase the yield surface will change and the current yield surface will be determined by

$$f(\sigma_{ij}, K^{\alpha}) = 0 \tag{3.37}$$

where the K^{α}, $(\alpha = 1, 2, ...)$, are hardening parameters that describe the way the yield surface change its size, shape and position with increased loading. The isotropic, kinematic and combined hardening models that are described bellow are defined by different hardening parameters.

Isotropic hardening
The yield surface in isotropic hardening keeps the position and shape while the size increase with plastic deformation described as

$$f = F(\sigma_{ij}) - \sigma_{y0} = 0 \tag{3.38}$$

where the σ_{y0} is the yield surface. The isotropic yield surface for a von Mises material is visualized in Figure 3.4. The specific isotropic hardening model used here is defined as

$$\sigma_{y0} = \sigma|_0 + Q_{\infty}(1 - e^{-b\bar{\varepsilon}^p}) \tag{3.39}$$

where $\sigma|_0$ is the initial yield stress when the plastic strain is zero [3]. The material parameters Q_{∞} is a value of the maximum increase of the yield stress and b explains the rate at which the maximum value of Q_{∞} is reached. This is calibrated from the test data that the user defines. The isotropic hardening model has the same yield stress in both compression and tension.

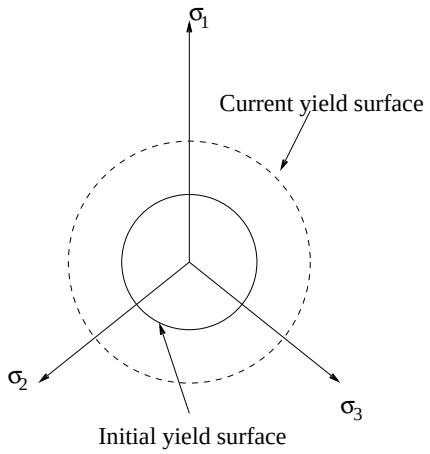

Figure 3.4: Isotropic yielding [5].

Kinematic hardening

The kinematic yield stress is not equal in tension and compression. This is called the Bauschinger effect. The yield surface in kinematic hardening moves its centre while the shape and size remain fixed with plastic deformation. The linear kinematic yield surface is defined by

$$f = F(\sigma_{ij} - \alpha_{ij}) = 0 \tag{3.40}$$

where α_{ij} is the back-stress tensor that describes the position of a yield surface in the stress space. The kinematic hardening model can be seen in

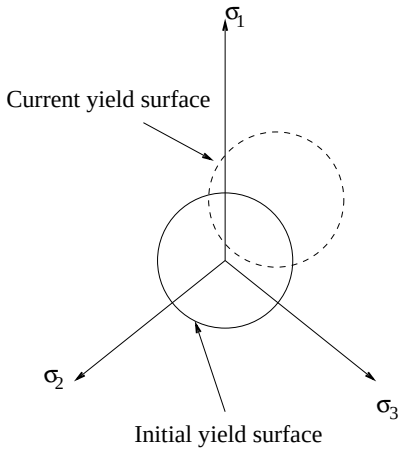

Figure 3.5: Kinematic yielding [5].

Figure 3.5 for a isotropic material. The evolution for the back stress tensor is based on Ziegler's hardening rule [3]

$$\dot{\boldsymbol{\alpha}} = C\frac{1}{\sigma_{y0}}(\boldsymbol{\sigma} - \boldsymbol{\alpha})\dot{\bar{\varepsilon}}^p \tag{3.41}$$

The components in (3.41) consists of the back-stress $\boldsymbol{\alpha}$, the back-stress rate $\dot{\boldsymbol{\alpha}}$, the size of the yield surface σ^0, the equivalent plastic strain $\dot{\bar{\varepsilon}}^p$ and the hardening parameter C. The initial yield surface is translated by the stress and back-stress tensors.

Combined hardening

The combined hardening model is a mix of isotropic and kinematic hardening defined by

$$f = F(\sigma_{ij} - \alpha_{ij}) - \sigma_{y0} = 0 \tag{3.42}$$

The yield surface will therefore change size and position while the shape will remain unchanged with plastic deformation, Figure 3.6. In ABAQUS

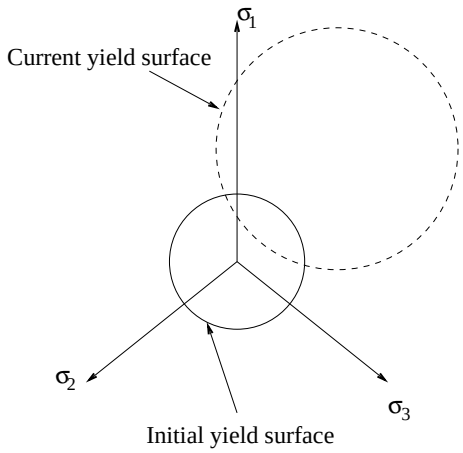

Figure 3.6: Combined yielding [5].

the combined hardening model is based on the non-linear kinematic and the isotropic hardening model, where the isotropic model is described by (3.39) and the kinematic [3] by

$$\dot{\boldsymbol{\alpha}} = C\frac{1}{\sigma_{y0}}(\boldsymbol{\sigma} - \boldsymbol{\alpha})\dot{\bar{\varepsilon}}^p - \gamma\boldsymbol{\alpha}\dot{\bar{\varepsilon}}^p \tag{3.43}$$

The nonlinearity is added in the kinematic hardening model (3.41) by the $\gamma\boldsymbol{\alpha}\dot{\bar{\varepsilon}}^p$ term in (3.43). Here γ is a material parameter. The combined hardening model is preferably used when cyclic loading is involved.

Chapter 4

Numerical solution method

This chapter will explain the numerical solution method. The FE-formulation will be defined as well as the computer program used in this thesis. The aim of the finite element method, FEM, is to solve problems where it is hard to determine an analytical solution. The FE-formulation is an method for solving arbitrary differential equations. The differential equation to solve is the equation of motion that is formulated as the principle of virtual power. This scalar equation will result in the FE-formulation. There are several different programs on the market based on this theory. The simulation program used in this thesis needs to handle large deformation since the soft material will deform considerable during impact. Another important parameter for the choice of simulation program is that nonlinear orthotropic material properties can be defined. It is also an advantage if the material can have orthotropic behaviour in both the elastic and plastic range. This combination of both elastic and plastic orthotropic behaviour is not very common today but is coming strongly. A simulation program that fulfils these requirements is ABAQUS. This simulation program is used to perform a large range of analyses. The main solvers are ABAQUS/Standard and ABAQUS/Explicit. These solvers will be explained further on in this chapter.

4.1 FE-formulation

The FE-formulation is built on the equation of motion (3.27) and will be written in matrix notation. At first the approximation of displacement is defined bellow as

$$\mathbf{u} = \mathbf{N}\mathbf{a} \tag{4.1}$$

where the interpolated displacement $\mathbf{u}$ is described by the shape function $\mathbf{N}$. From this equation the acceleration vector is easy to derive and is presented as

$$\ddot{\mathbf{u}} = \mathbf{N}\ddot{\mathbf{a}} \tag{4.2}$$

The approximations above is used to compute the deformation rate as

$$\mathbf{D}^v = \mathbf{B}\mathbf{a} \tag{4.3}$$

where the $\mathbf{b}$ contains the derivative of the shape functions. From the Galerkin method [4] the weight function is determined as

$$\mathbf{w} = \mathbf{N}\mathbf{c} \tag{4.4}$$

Using (4.1)-(4.4) in (3.27) the following equation is obtained

$$\mathbf{c}^T \left(\int_V \rho \mathbf{N}^T \mathbf{N} \ddot{\mathbf{a}} dV + \int_V \mathbf{B}^T \boldsymbol{\sigma} dV - \int_S \mathbf{N}^T \mathbf{t} dS - \int_V \rho \mathbf{N}^T \mathbf{b} dV \right) = 0 \tag{4.5}$$

Now the FE-formulation starts to appear

$$\int_V \rho \mathbf{N}^T \mathbf{N} dV \ddot{\mathbf{a}} + \int_V \mathbf{B}^T \boldsymbol{\sigma} dV - \int_S \mathbf{N}^T \mathbf{t} dS - \int_V \rho \mathbf{N}^T \mathbf{b} dV = 0 \tag{4.6}$$

where $\mathbf{M}$, $\mathbf{f}_{int}$ and $\mathbf{f}_{ext}$ are matrixes defined as

$$\mathbf{M} = \int_V \rho \mathbf{N}^T \mathbf{N} dV \tag{4.7}$$

$$\mathbf{f}_{int} = \int_V \mathbf{B}^T \boldsymbol{\sigma} dV \tag{4.8}$$

$$\mathbf{f}_{ext} = \int_S \mathbf{N}^T \mathbf{t} dS - \int_V \rho \mathbf{N}^T \mathbf{b} dV \tag{4.9}$$

This results in the general FE-formulation

$$\mathbf{M}\ddot{\mathbf{a}} = \mathbf{f}_{ext} - \mathbf{f}_{int} \tag{4.10}$$

4.2 Implicit vs explicit code formulation

In this section the implicit and explicit code formulation will be compared to each other. ABAQUS/Standard can solve a wide range of various linear and nonlinear problems by using an implicit time integration scheme. This

means that the program iterate using the gradient of the next point to determine an acceptable solution. The slope of the function $f(t)$ to the next time point t is illustrated in Figure 4.1. The implicit calculation method often iterate several times before an acceptable equilibrium has been found. The implicit calculation method is not suitable for dynamic impact prob-

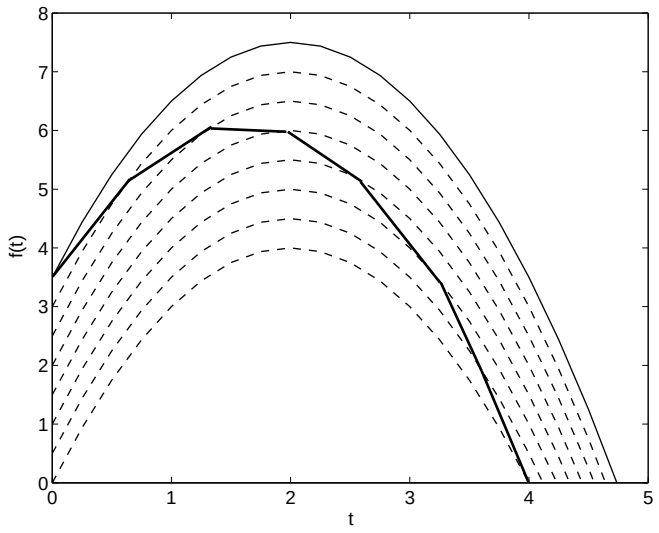

Figure 4.1: Implicit calculation method [7].

lems where contact is involved, in those cases ABAQUS/Explicit is recommended. This method is used for large deformation that occurs during a short time. ABAQUS/Explicit applies the explicit time integration method, meaning that the last increment is used to anticipate the next step. In Figure 4.2 the gradient of the start point is used to determine the function $f(t)$ of the next time step t. The main difference between ABAQUS/Standard and ABAQUS/Explicit is that the implicit method iterate while the explicit method anticipate every step. The implicit method is always stable whereas the explicit method is conditionally stable. This leads to that the disk space and memory usage is much higher in ABAQUS/Standard analyses [3]. ABAQUS/Explicit is suitable for the application in this thesis considering that the program is used for large deformation analysis with a short time duration.

4.3 Explicit calculation method

The explicit method is very efficient for problems with short load duration for example in impact problems and explosions. ABAQUS/Explicit uses the

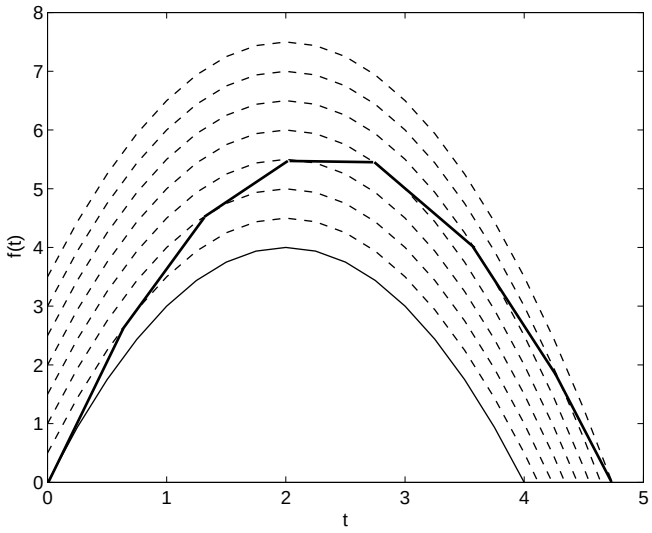

Figure 4.2: Explicit calculation method [7].

explicit central-difference integration rule to integrate the equation of motion for a body [3]

$$\mathbf{M}\ddot{\mathbf{u}}^{(\mathbf{i})} = \mathbf{f}_{ext}^{(i)} - \mathbf{f}_{int}^{(i)} \tag{4.11}$$

The equation of motion is used to calculate the nodal acceleration $\ddot{\mathbf{u}}$ at every time step using the diagonal mass matrix $\mathbf{M}$, the applied load vector $\mathbf{f}_{ext}$ and the internal force vector $\mathbf{f}_{int}$. The benefit of the diagonal mass matrix is that the computational effort is reduced since the accelerations are solved directly as

$$\ddot{\mathbf{u}}^{(i)} = \mathbf{M}^{-1} \cdot (\mathbf{f}_{ext}^{(i)} - \mathbf{f}_{int}^{(i)}) \tag{4.12}$$

and therefore requires no iterations. This calculation is performed at the beginning of every increment. Further the acceleration is used to calculate the velocity at the next time step

$$\dot{\mathbf{u}}^{(i+\frac{1}{2})} = \dot{\mathbf{u}}^{(i-\frac{1}{2})} + \frac{\Delta t^{(i+1)} + \Delta t^{(i)}}{2}\ddot{\mathbf{u}}^{(i)} \tag{4.13}$$

This requires that the initial velocity, $\dot{\mathbf{u}}^{(\mathbf{i}-\frac{\mathbf{1}}{\mathbf{2}})}$, is determined. When the velocity is determined, the displacement can be calculated according to

$$\mathbf{u}^{(i+1)} = \mathbf{u}^{(i)} + \Delta t^{(i+1)}\dot{\mathbf{u}}^{(i+\frac{1}{2})} \tag{4.14}$$

At the first time step t=0 the velocity, $\dot{\mathbf{u}}^{(0)}$, and the acceleration, $\ddot{\mathbf{u}}^{(0)}$, is defined by the user or is set to zero. To be able to use (4.13) and (4.14) the $\mathbf{u}^{(+\frac{1}{2})}$ and $\mathbf{u}^{(-\frac{1}{2})}$ need to be calculated. This is done in the following equations

$$\mathbf{u}^{(+\frac{1}{2})} = \dot{\mathbf{u}}^{(0)} + \frac{\Delta t^{(1)}}{2}\ddot{\mathbf{u}}^{(0)} \tag{4.15}$$

$$\mathbf{u}^{(-\frac{1}{2})} = \dot{\mathbf{u}}^{(0)} - \frac{\Delta t^{(1)}}{2}\ddot{\mathbf{u}}^{(0)} \tag{4.16}$$

The following steps in the explicit calculation are to determine the strain increments in the elements and then the stresses. Finally the internal forces can be computed. Now the next integration step can be performed. The disadvantage with an explicit method is that small errors are introduced with time in the solution, which can make the solution unstable [5]. To avoid this, the time increment has to be within a certain range. The time increment should be small enough that the acceleration within the increment is constant. In ABAQUS/Explicit the stable time step with damping is obtained with

$$\Delta t \leq \frac{2}{\omega_{max}}(\sqrt{1+\xi^2} - \xi) \tag{4.17}$$

where ξ is the fraction of critical damping in the highest mode [3] and ω_{max} is the highest frequency in the system. A small amount of damping is introduced as bulk viscosity in ABAQUS/Explicit. This is done to improve the modelling of high-speed dynamic solutions because bulk viscosity introduces damping associated with the volumetric straining [3]. The time step depends on if the FE-model contains one or several materials. When there is only one material the time increment is directly proportional to the size of the smallest element in the mesh. In uniform meshes with several materials the initial time increment depends on the highest wave speed in the elements. The wave speed c_d is determined by Young's modulus E and the mass density ρ as.

$$c_d = \sqrt{\frac{E}{\rho}} \tag{4.18}$$

Further ABAQUS/Explicit uses two strategies for supervising the time step, either calculating a new time increment or using a fixed time step. The wave speed c_d and the smallest dimension L_{min} in the mesh is used to get an approximation of the stable time step.

$$\Delta t \approx \frac{L_{min}}{c_d} \tag{4.19}$$

There are analyses that are nearly impossible to run since they require enormous amount of time to solve. One way to FE-simulate a time demanding

problem is to increase the mass of the part, so called mass scaling. The theory behind this solution are based on the equation (4.18) and (4.19). If the density ρ increases the wave speed c_d will decrease. This leads to that the stability limit Δt increases which will result in a shorter solution time. The mass scaling will have influence on the inertia effects therefore the results needs to be controlled to see that the inertia effects have not jeopardized the solution. Unfortunately it is not possible to mass scale the FE-model in this thesis since this is not compatible with the EOS-formulation, used for modelling the water. The EOS-formulation will be discussed in chapter 6.2.

4.4 Energy balance

When using explicit integration methods it is necessary to control the energy balance. As already mentioned the explicit integration method can introduce small errors if the time increment is too large. To verify if the solution is accurate the energy values can be examined. The energy balance is defined in

$$E_I + E_V + E_{FD} + E_{KE} - E_W = E_{Total} = \text{constant} \tag{4.20}$$

where E_I is the internal energy, E_V is the viscous energy dissipation, E_{FD} is the friction energy dissipation, E_{KE} is the kinetic energy and E_W is the work done by externally applied loads. The energies in (4.20) results in the total energy, E_{Total}. A good way to verify the solution is to investigate if the total energy is constant during the cause of the simulation. The total energy term is constant since the energy can not disappear only be transformed. In numerical methods the solution is not completely constant but should not vary by more than 1% [3]. The internal energy is the sum of the energies defined by

$$E_I = E_E + E_P + E_{CD} - E_A \tag{4.21}$$

where E_E is the recoverable strain energy, E_P is the energy dissipated through inelastic processes such as plasticity, E_{CD} energy dissipated through viscoelasticity or creep and E_A is the artificial strain energy. The artificial energy is a measurement of energy stored in hourglass resistant and transverse shear in shell elements. If the artificial energy is large the mesh should be improved [3].

Chapter 5

Experimental test methods

To verify the simulations different experimental test methods are used to examine if a correlation between a certain test method and the simulations exist. The aim is to find a parameter that can be evaluated in the simulation. Two different test methods are considered in this thesis, i.e. drop test and energy fracture test with dynamic pendulum. Both these methods are practiced at Tetra Pak R&D but the dynamic pendulum will be applied for a different purpose than usually used.

5.1 Drop test

The drop test method is a very simple test method and corresponds well to the reality. The disadvantage with this method is that the test only results in an intact or damaged package. There are no parameters that actually tell how good the package resists an impact. The impact velocity of the package is a crucial parameter since large forces affect the package during a short tome. The impact velocity is dependent of the drop height. The impact position of the package when hitting the ground is another parameter that can be investigated since all packages do not behave in the same way during impact. The position of the package before impact is difficult to see with the bare eye since the total impact in a drop test occurs in less than 200 ms. Further the method is time demanding since several packages have to be dropped to get an indication of what height a package can handle. The parameters that are tested are different package material and sealing types. Every time these parameters change, a test series of 200 packages are dropped at 4-5 different heights. Package materials and sealings that manage a high drop height are evaluated further. The improvements are continued until the package reach a satisfactory height established by the development group.

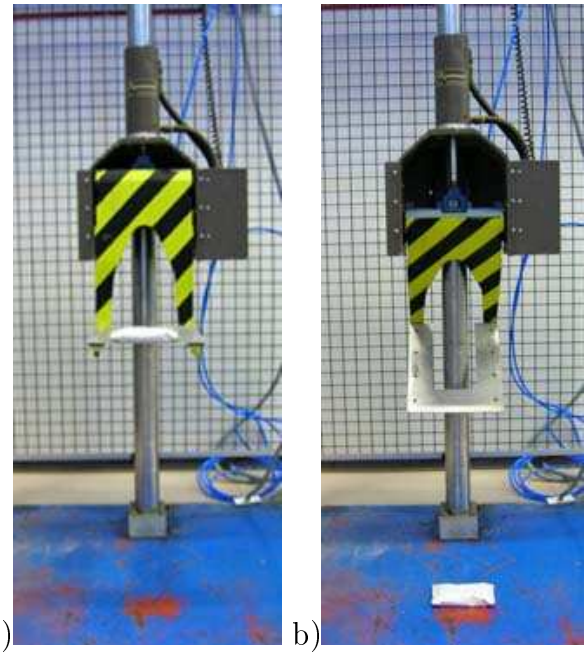

Figure 5.1: Drop test equipment a) initial position and b) final position.

5.1.1 Experimental setup

The drop test is performed as a fall from rest. The package is placed on a fork at a desired height. The fork is withdrawn very fast and the package falls to the ground. Then the package is evaluated against certain leakage criteria, namely if the leaking has started in the package material or at the sealings. The side with the longitudinal sealing is always put upwards in a standard drop test at Tetra Pak R&D. This fall will be called horizontal position in this thesis. In this thesis the drops are filmed with high-speed camera to capture the package behaviour during impact. Packages, at various heights, will be filmed from above and from the long side. A fall where a transversal sealing will hit the ground first will also be filmed. The package is dropped manually to get the right orientation in this fall. This fall will be called a vertical fall further on in this thesis.

5.1.2 Result

The result from the drop test indicates that the area around the transversal sealing is critical since the sealings fracture sometimes. Another crucial parameter is the packaging material, if the material fractures it usually occurs on the impact side of the package.

Figure 5.2: A material crack in a package.

The high-speed films made it possible to see how the package behaves during impact. The first observation was that it is very difficult to receive an entirely horizontal impact position. The packages usually have an angular velocity or rotation that results in an impact that is difficult to analyze. This leads to that the deformation behaviour in the high-speed films depends on the impact position. The vertical fall was a bit easier to film since the package has its mass close to its centre of gravity. The result of the high-speed films will be used to evaluate the FE-simulated analysis further on in chapter 8.

5.2 Dynamic pendulum

The dynamic pendulum measures the energy absorption in a sample. This test method brings a measurement on the contrary from the drop test method. The dynamic pendulum test does not correspond to the reality as well as the drop test method but it gives energy absorption levels that classifies different materials. Another reason to evaluate this method is the fact that it is a dynamic method like the drop test. The dynamic pendulum test is performed on a sample of the transversal sealing in this thesis but it is usually performed on a material sample. The transversal sealing is tested with the dynamic pendulum since it is near this area the damage is detected. The expectation for the dynamic pendulum test is to detect differences in the material properties or the sealings and to obtain a parameter that can be used in the simulation.

Figure 5.3: Dynamic pendulum test equipment.

5.2.1 Experimental setup

A pendulum that corresponds to the energy level of 0.5 J is positioned at a fixed height. Then a sample is positioned between two jaws, one fixed and one movable. The pendulum is dropped and hits the moveable jaw. The sample cracks into two pieces. The pendulum measures the energy that is required to crack the sample. The sealings are tested with the dynamic pen-

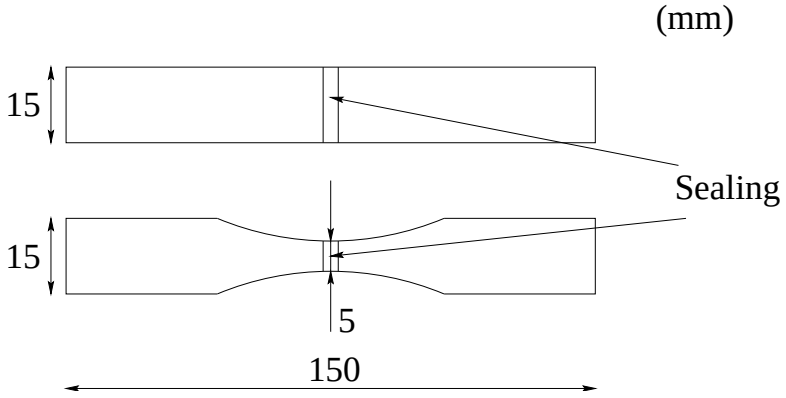

Figure 5.4: Two sample geometries tested in the dynamic pendulum.

dulum since the drop test indicates that transversal sealing is a weakness in the aseptic pouch. Three test sets were performed.

In the first test set with the pendulum different parameters were tested to get an idea of which ones that made a difference in the result. The tested parameters were different shapes of the samples and sealing types, according to Figure 5.4. A comparison was also performed between the top and bottom sealing. All the samples in the first set were conditioned at 23°C and 50% air humidity.
In the second test set different material types were tested. The samples were conditioned at 23°C but at two different air humidities, 50% respectively 80%.
The last set of tests was performed at TFA-packages that actually had huge differences in the drop test. This test was performed with the samples conditioned 23°C and 50% air humidity since paperboard properties depends on the humidity.

5.2.2 Result

In the first test setup there was no significant difference between the sealing types. No differences were detected when the shape of the sample according to Figure 5.4 was considered in the evaluation process. The energy levels were a bit higher in the 15 mm samples than in the 5 mm samples but they were not three times higher as expected. The test did not discover any actually difference in the energy absorption. After this set a decision was made to only use the 5 mm samples since these were easier to prepare. In the second test setup where the humidity was changed no significant differences could be detected. The result is showed in Figure 5.5. At last different TFA materials were tested. The result shows that there are no significant differences between these TFA package materials in the sealing. The energy absorption levels in the TFA materials are about the same. Both materials absorb energy around 0.20 J to 0.23 J. This can be compared to the energy levels in the sealing of the aseptic pouch that measures 0.16 J to 0.21 J at 50% air humidity. The total outcome from these results is that the dynamic pendulum did not detect differences in the sealings. Another result is that the pendulum could be too heavy for these types of packaging materials. The energy levels that are measured with the 0.5 J pendulum are in the interval 0.16 J to 0.23 J. The pendulum has twice the energy that was needed to crack the samples.

5.3 Discussion

The drop test method corresponds to the reality but it does not give any measures. The procedure of high-speed filming the impact during the drop

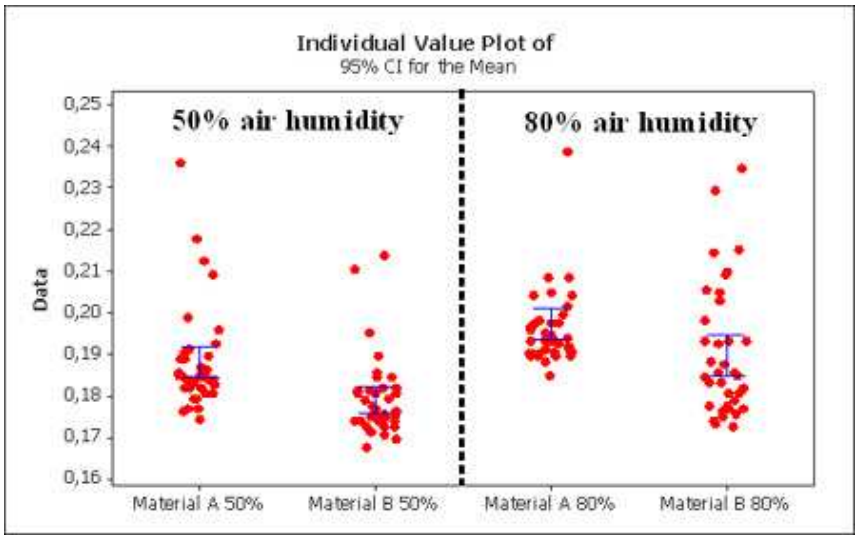

Figure 5.5: Energy absorbtion for the samples tested with various humidity.

test gives the opportunity to evaluate the simulation by comparing the behaviour between the simulated and high-speed filmed package.
The dynamic pendulum method has been tested on the transversal sealings for the aseptic pouch and TFA, since one of the critical areas are around the sealing. The outcome of the tests shows that there are no significant differences between the sealings, not even when the samples were treated in higher humidity.
The result of the dynamic pendulum tests shows that the pendulum energy is twice of the energy absorption in the sample. It could be interesting to try a pendulum with a smaller energy level, perhaps around 0.20 J to be able to see significant differences in the sealings.

Chapter 6

Material models

The material model that will be assigned in the FE-simulation will be established in this chapter. The packaging material has orthotropic properties in both the elastic and plastic region. It is possible to assign both orthotropic elasticity and plasticity in ABAQUS 6.5. This has not been possible in earlier versions. The problem in this thesis contains large deformation, it is therefore important that the material is properly defined in the plastic region. The properties of the water inside the package will be established by an equation of state, EOS.

6.1 Packaging material

The procedure to determine the material parameters for elastic and plastic behaviour as well as the hardening models will here be described in detail. The packaging material is a laminate containing paperboard and polymers. The paperboard gives the laminate its orthotropic properties. In this thesis the material parameters will be determined for the entire laminate and not for each layer. The material data is obtained from tensile tests performed on the packaging material in both MD and CD. As apparent from the tensile curves in Figure 6.1 there are large differences between the two directions. MD can handle higher strength while CD has better strain capability. The ZD properties are situated in the out of the plane direction and the strength in this direction is much smaller than the other directions for paperboard. The packaging material that is used in this thesis is not available on the market and therefore the measures are not shown in the tensile graphs in Figure 6.1 and Figure 6.3-6.5.

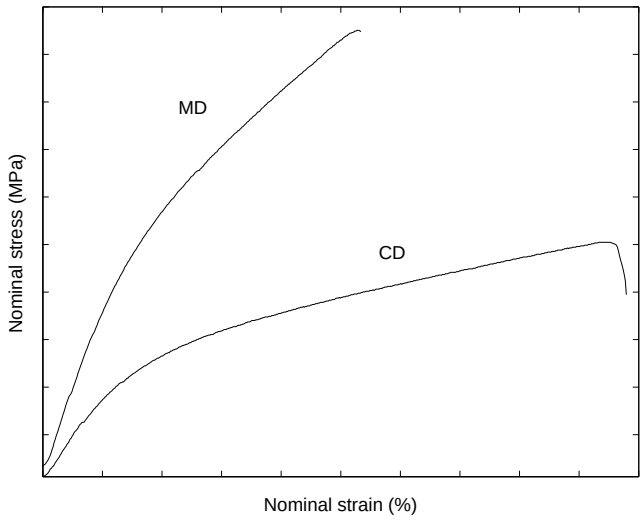

Figure 6.1: Test data for the packaging material in machine and cross machine direction.

6.1.1 Orthotropic elastic parameters

A material enters the elastic region when it is loaded and no permanent strain occurs. The material responds elastically until it reaches the yield stress, σ_{yo}. In the elastic region the Young's modulus E is determined. To obtain a proper material model with orthotropic properties the Young's modulus is determined for MD and CD. The orthotropic properties of the material can be defined in ABAQUS in several ways. One of them is to define the elastic engineering constants for the material. The parameters are established by considering a tensile strain curve for the material. The orthotropic constitutive relation between stress and strain is defined according to

$$\boldsymbol{\varepsilon} = \boldsymbol{C}\boldsymbol{\sigma} \tag{6.1}$$

where $\boldsymbol{\varepsilon}$, $\boldsymbol{C}$ and $\boldsymbol{\sigma}$ are defined as

$$\begin{bmatrix} \varepsilon_{11} \\ \varepsilon_{22} \\ \varepsilon_{33} \\ \gamma_{12} \\ \gamma_{13} \\ \gamma_{23} \end{bmatrix} = \begin{bmatrix} \frac{1}{E_{11}} & \frac{-\nu_{12}}{E_{13}} & \frac{-\nu_{13}}{E_{33}} & 0 & 0 & 0 \\ \frac{-\nu_{12}}{E_{11}} & \frac{1}{E_{22}} & \frac{-\nu_{23}}{E_{33}} & 0 & 0 & 0 \\ \frac{-\nu_{13}}{E_{11}} & \frac{-\nu_{23}}{E_{22}} & \frac{1}{E_{33}} & 0 & 0 & 0 \\ 0 & 0 & 0 & \frac{1}{G_{12}} & 0 & 0 \\ 0 & 0 & 0 & 0 & \frac{1}{G_{13}} & 0 \\ 0 & 0 & 0 & 0 & 0 & \frac{1}{G_{23}} \end{bmatrix} \begin{bmatrix} \sigma_{11} \\ \sigma_{22} \\ \sigma_{33} \\ \sigma_{12} \\ \sigma_{13} \\ \sigma_{23} \end{bmatrix} \tag{6.2}$$

where the 1-, 2- and 3 corresponds to MD, CD and ZD. The material engineering constants will be defined in this section. The Young's modulus is

determined by calculating the slope of the tensile-strain curve in the elastic region. The yield stress for MD is estimated from numerous test curves since the yield point is not distinguished in the graph. The Young's modulus is decided in the same way for MD and CD. The relations that Baum [8] established are used to decide the Young's modulus in ZD and the shear modulus. These relations are established for paperboard properties and not for a laminate structure with polymers. The relations will here be used anyway since is assumed that the dominant properties in the laminate are received from the paperboard.

$$E_3 = \frac{E_1}{200} \tag{6.3}$$

$$G_{12} = 0.39\sqrt{E_1 E_2} \tag{6.4}$$

$$G_{13} = \frac{E_1}{55} \tag{6.5}$$

$$G_{23} = \frac{E_2}{35} \tag{6.6}$$

6.1.2 Orthotropic plastic parameters

Plasticity is one of the stages that many materials pass when loaded to fracture. From the yield point the material develops plastic strains. These strains will remain even after unloading the material. If the load increases the plastic behaviour will continue until the material fractures. This behaviour is shown in Figure 6.2. The total strain is a combination of the elastic, ε^e, and plastic strain, ε^p.

$$\varepsilon_{ij}^t = \varepsilon_{ij}^e + \varepsilon_{ij}^p \tag{6.7}$$

This formulation is only stated for small deformations but will here be used to establish the plastic strains. In ABAQUS/Explicit the plastic behaviour of a material is described by assigning true stresses and true plastic strains according to Cauchy theory. These are obtained from a stress-strain curve by converting the nominal measures. Nominal measures are calculated on an undeformed geometry while the true values depends on a deformed geometry. The true measures can be determined by using following relations

$$\varepsilon^{true} = ln(1 + \varepsilon^{nom}) \tag{6.8}$$

$$\sigma^{true} = \sigma^{nom}(1 + \varepsilon^{nom}) \tag{6.9}$$

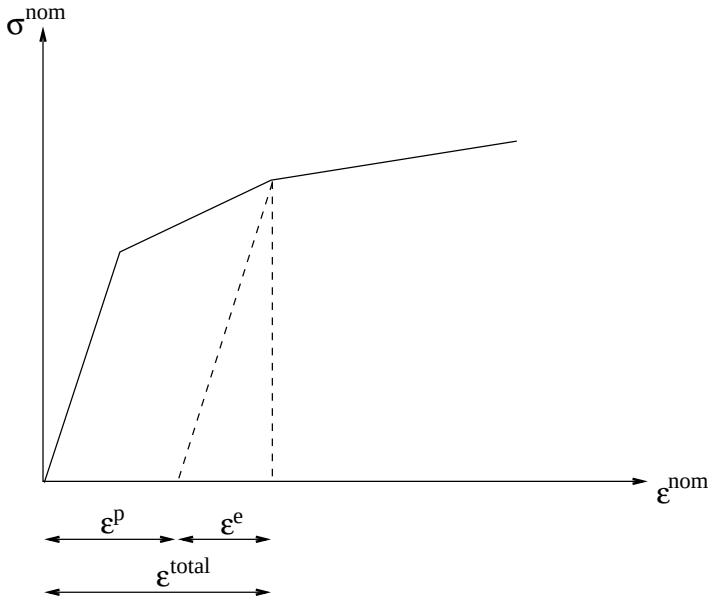

Figure 6.2: Tensile curve showing ε^e, ε^p and ε^{total}.

$$\varepsilon^p = \varepsilon^{nom} - \varepsilon^e = \varepsilon^{nom} - \frac{\sigma^{true}}{E} \tag{6.10}$$

The orthotropic behaviour in the material is obtained by using Hill potential, see section 3.3.1.

6.1.3 Verifying hardening models

Three hardening models in ABAQUS/Explicit, according to section 3.3.2, are compared to decide which model that fits the experimental tensile test data the best. The hardening models that will be examined are isotropic, linear kinematic and combined hardening model. A simple tensile test is simulated to verify the hardening material models. When this is done the material model can be implemented in the FE-simulation of a dropped package. The tensile test is simulated similarly to the execution of the experimental test. In the FE-simulation the sample has the same geometry as the sample in the practical tensile test. The sample has a rectangular geometry and contains only one shell element. The material parameters are implemented as engineering constants for orthotropic elastic behaviour. To establish the plastic behaviour Hill potential is used to define the orthotropic properties with different hardening models. Plane stress is used since the problem is two-dimensional. The sample is fixed at one short end in the loading direction

and can not be rotated. The opposite end is displaced. The displacement is applied as a ramped function defined by an amplitude curve to prevent chock loading in the sample. Two tests are performed since the material possesses orthotropic properties. In the first test the displacement is applied in the machine direction and in the other test in the cross machine direction. To verify that the material model behaves properly, the stress-strain curves from the FE-simulation and the tensile test are compared. When simulating in ABAQUS/Explicit the calculations are performed on deformed geometry. The practical tensile test data are calculated per default on the nominal geometry, see section 3.1.3. A FE-simulation was performed on both nominal and true geometry. The default setting in ABAQUS is to calculate on true geometry. The differences were small and therefore assumed to be negligible. The hardening is implemented from experimental data points according to section 6.1.2. The data points should not be too many or have a large number of decimals since this makes it harder to adjust a curve. The material curve is calculated to be adjusted to the material input data. To establish the isotropic or combined material model several data points are required while the linear kinematic model only is defined by two points namely the initial yield stress and the end point. The result of the simulated tensile test is shown in Figure 6.3-6.5.

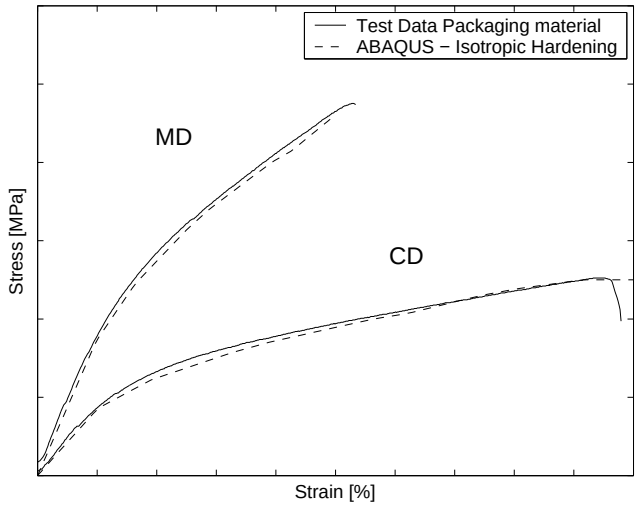

Figure 6.3: Calibration of a material curve with isotropic hardening in ABAQUS.

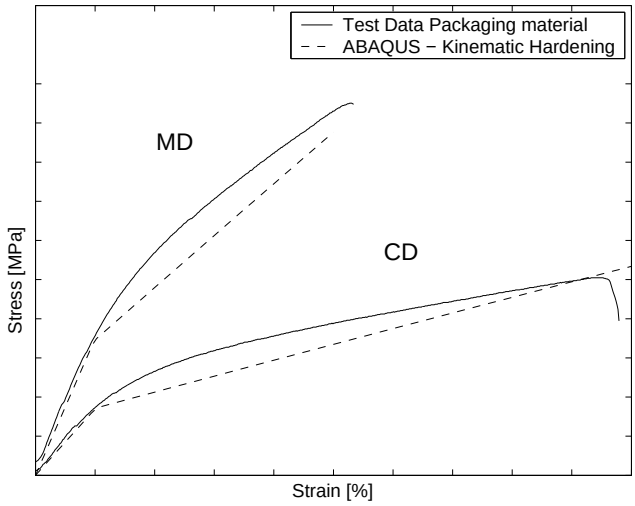

Figure 6.4: Calibration of a material curve with linear kinematic hardening in ABAQUS.

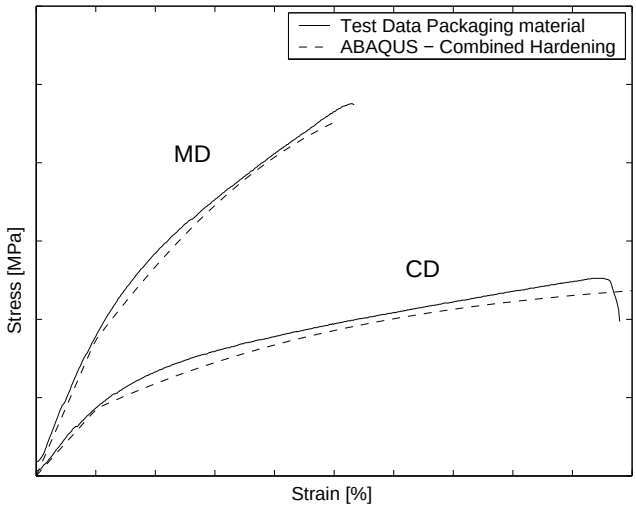

Figure 6.5: Calibration of a material curve with combined hardening in ABAQUS.

6.1.4 Conclusion

The results from the verification of the hardening models shows that the isotropic hardening model corresponds best to the experimental test data. The combined model fits the test data well but is primarily used in cyclic loadings. The kinematic curve just approximates a linear hardening model. This suites problem exposed to large tensile stresses that transforms into compression stresses. The isotropic hardening model is chosen since it suits the experimental tensile curves the best. The material model contains orthotropic elasticity and isotropic hardening with Hill potential that will provide orthotropic properties.

6.2 Fluid material

In ABAQUS/Explicit an equation of state, EOS, can be used to model water as a hydrodynamic material. This is done to give the solid elements its fluid properties. In this case a linear equation of state is used for the product in the package, that is as mentioned earlier the water. The linear EOS in ABAQUS/Explicit describes a linear relation between volumetric strain and pressure. When defining EOS three parameters are required, c_0, s and Γ_0. The c_0 parameter is the speed of sound in the fluid and can be determined by

$$c_0 = \sqrt{\frac{K}{\rho}} \tag{6.11}$$

where K is the bulk modulus and ρ is the density. This only applies for a fluid with small compressibility [9]. The fluid is assumed to be incompressible but is approximated to have small compressibility. The bulk modulus for water is defined as $K = 2.2$ GPa and $\rho = 1000$ kg/m^3 [10]. This results in a speed of sound $c_0 = 1483$ m/s. The material parameters s and Γ_0 are both non-dimensional and are defined as zero on recommendation from ABAQUS-support since the fluid is incompressible and non-viscous. A better way to FE-simulate the fluid behaviour is to use computer software, like CFDesign, that is more suitable for fluid solutions.

Chapter 7

FE-modelling in ABAQUS

The FE-simulations will be performed on an aseptic pouch filled with liquid to investigate whether it is possible to imitate the behaviour of a fluid inside a soft beverage package during impact. This to analyse in which way the packaging material is affected. The difficulties with the analysis are to obtain a good geometry, correct material parameters and decide which parameters to evaluate. The FE-simulation will be performed in the computer program ABAQUS. The program contains several interacting softwares for instance ABAQUS/CAE and ABAQUS/Viewer. ABAQUS/CAE stands for Complete ABAQUS Environment and is a pre-processor. CAE is a graphical environment where models can be created or imported from other CAD-systems. ABAQUS is divided into ten modules to facilitate the use of the pre-processor. The modules are part, property, assembly, step, interaction, load, mesh, job, visualization and sketch according to Figure 7.1. ABAQUS/Viewer is a postprocessing tool that visualizes the result of an analysis. This chapter describes the modelling procedure for a package that

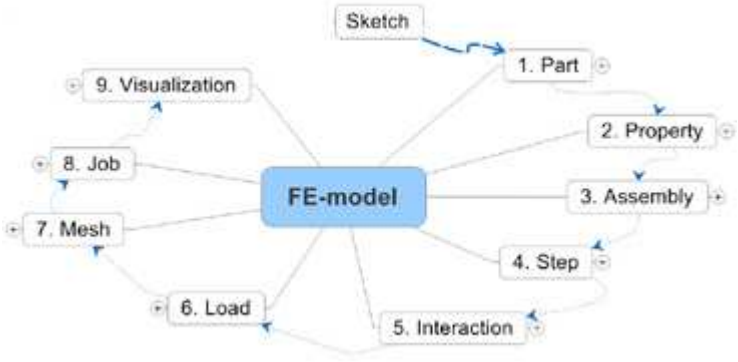

Figure 7.1: A scheme of the modules in ABAQUS/CAE.

is exposed to a free fall. This drop test analysis contains three model parts; a package, a fluid-geometry and a floor. The package with the fluid inside is dropped on a rigid floor. To get an idea of how accurate the FE-simulations correspond to reality, high-speed films of real drop tests are consulted. The FE-simulations will later be verified in the visualization module against high-speed films to see if the deformation behaviour is similar.

7.1 Modelling procedures

The shape of the package that is studied in this thesis is very simple since the package only is a pouch filled with liquid. The modelling procedure is a bit more difficult. One way to model the structure is to use several ellipses with different size as presented in Figure 7.2. The ellipses are used as a base when lofting the fluid volume. The lofting command calculates curves between the ellipses and connects them together. One of these curves is illustrated in Figure 7.2. Every point on the ellipse has its own curve. Together the curves can create a volume or an area.

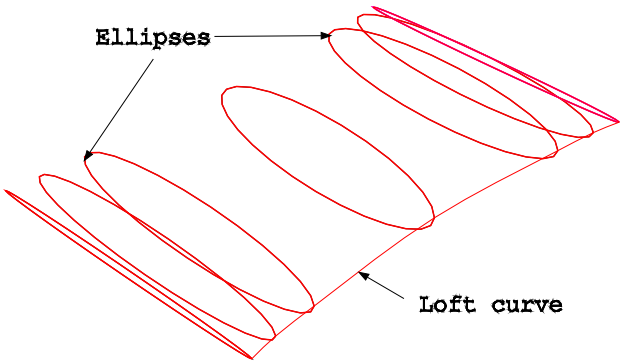

Figure 7.2: Ellipses defining the package geometry.

At first a solid part is created with the loft procedure that represents the fluid in the FE-model. To verify the geometry of the fluid, three parameters are examined

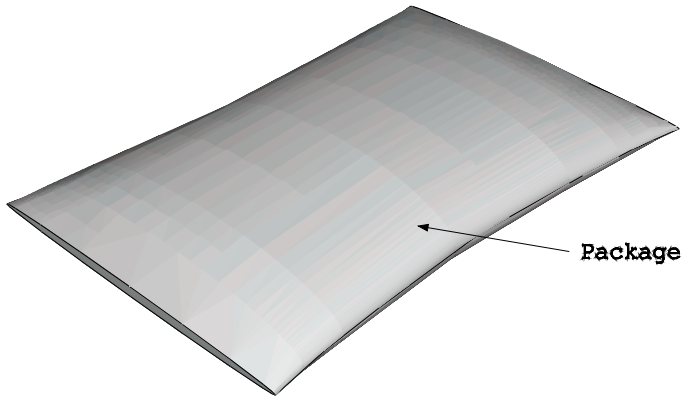

Figure 7.3: Package created with loft.

- the circumferences of the ellipses are checked. All the ellipses should have approximately the same circumference as the tube has during the filling process since it is this tube that is sealed into a package.
- the volume of the solid is verified to be 250 cm^3 since the package contains 250 ml.
- the mass of the entire FE-model can be verified to 0.254 kg which is the average weight of the package with water inside.

The geometry of the fluid ends can be represented as straight lines since the tube is squeezed together. When performing the solid loft operation between the ellipses and the straight lines a problem occurs. The solid loft operation disapproves this kind of loft. The modelling procedure for the sealings will be described further on in this chapter. The package is totally filled with fluid which means that there are no cavities. This is a very important aspect to introduce into the simulation. In this thesis three different modelling techniques were considered to create the fluid and package interaction. The first alternative is to create a package part from the outer surface of the fluid part and then assign contact definition between the fluid and the inner surface of the package. This is the most common technique when modelling contact conditions. Unfortunately this technique is not proper for this FE-model since it was discovered at an early stage that the fluid and the package did not interact very well since cavities occurred between the package and the

fluid. This option will therefore not be further investigated in this thesis. The second option is to improve the interaction between the fluid and the package to prevent the cavities that occurred in the previous method. This will be done by merging the nodes from the two parts at the interacted surfaces. The merging nodes modelling technique will be described further in the next section. In the third method the package material was created based on the skin option that were found in the property module in ABAQUS/CAE. The skin operation is actually performed on the solid mesh of the fluid part and creates a shell mesh representing the package. The skin modelling procedure will also be discussed in detail in this chapter.

7.1.1 Model with merged nodes

This section will cover the modelling procedure with merged nodes. As mentioned the package was created from the solid fluid part. A copy is made of the solid part and then converted to the package shell part. This is an easy task to perform in the part-module. The choice of a shell part is based on the fact that the packaging material is very thin and therefore well suited for shell elements. Further the parts are assembled, the fluid is placed inside the package. Since the fluid and the package have the same size the fluid is kept inside by the contact definition *constraints with *ALL*. This command makes sure that all parts are in contact with each other. The package and the fluid are meshed in a similar way but with different types of elements, shell respectively solid elements. An equal mesh can be accomplished if both parts are partitioned and seeded in the same way. With the seed operation the element mesh can be controlled by the element size or by number of elements in a region. The purpose with the equal meshes is to enable merging the nodes. The nodes will be merged at the interacting surfaces between the fluid and the package. This procedure leads to that some elements share nodes with each other but still keep their own element properties. In spite of the fact that the meshes are divided in exactly the same way the nodes will not match perfectly in the assembly. The reason is that when partition the parts the loft curve will be split and the entire shape changes in different ways for the solid and shell parts. When splitting a loft curve the number of interpolation points decrease and the curve gets a different appearance. There will be a difference between the shell and the solid part since the loft procedure calculates volumes and surfaces differently. This causes problems in the merging operation since the element nodes do not match perfectly with each other for the different parts. In the merging procedure a tolerance of the largest distance that is allowed between the nodes is set. Only nodes in the tolerance range will be merged. Observe that the tolerance range should

not be larger than the smallest side of an element because then nodes within one element will be merged. In this case the tolerance should not be larger than 0.05 mm. Notice that when a merge node procedure is performed an entirely new part is created containing only an orphan mesh with its elements. This means that material properties and boundary conditions must be assigned for the new mesh part. The materials and boundary conditions will be described in further sections.

7.1.2 Model with skin

In this section the modelling procedure of the package with the skin operation in ABAQUS/CAE will be described. At first the solid part is assigned its fluid properties and then the skin is positioned on the surface of the part. When creating a skin in the property-module, shell and material properties are assigned to the skin region. The surface of the shell elements coincide with the upper surface of the fluid elements. The part is then assembled with the floor. The meshing procedure is performed by partitioning and seeding the fluid part. The fluid part is assigned an explicit solid element type and the skin is assigned an explicit shell element type. Then the fluid part is meshed, equal shell respectively solid elements and nodes positions appear in the part at the skin region. The skin is symbolizing the package and is interacting with the fluid inside since the nodes are shared between the solid and shell elements at the surface.

7.1.3 Choice of simulation model

It is now time to evaluate the modelling procedure and choose the most suitable technique. When comparing the models it was found that the modelling procedure with skin has major benefits compared to the merge node method. The skin method is easy to use and fewer parts have to be created. The benefit with one part is that it facilitates when changing parameters in the package geometry since the changes only have to be performed in one part. When performing a geometry change in the merge node FE-model, it has to be done in both the fluid and package parts and then the entire merge procedure must be performed all over again. The fact that the meshes match entirely which eliminates the cavities is another benefit with the skin modelling. In the FE-model with merged nodes cavities occurs during the simulation since not all nodes at the surfaces are merged. As apparent the skin FE-model is to prefer, but it can be mentioned that it has its backsides too, especially when assigning the material orientation. When the material orientation is assigned to the skin it can not be verified if the orientation is

properly applied before submitting the job. This is only possible to check in ABAQUS/Viewer after submitting a job. The material orientation check is easy to perform in a shell part, which is the case in the merging model. The possibility to visualize both fluid and package in a cut plane position is an advantage for the merge node FE-model. The result of this evaluation is that the skin FE-model is to prefer. The combination of easy modelling procedure and good interaction behaviour between the fluid and package makes the skin modelling procedure to the preferred modelling strategy. In the next section the development of a final FE-model with the transversal sealing is described.

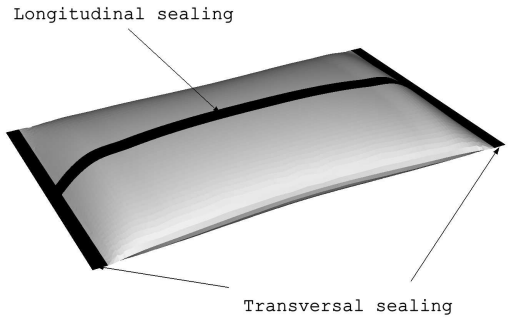

Figure 7.4: Longitudinal and transversal sealings in the package.

7.1.4 Sealings in the FE-model

The final FE-model will be built up with the skin operation and the two sealing types will be added according to 7.4. The transversal sealing will be approximated to a rectangular shell element piece with double thickness at each short side. As mentioned the solid loft operation does not approve with letting a solid loft end with a straight line. The lofting will therefore be performed as a shell loft and then converted to a solid part. This operation is performed to avoid the cavity. The lofting is performed from a straight line through the ellipses and ends in a straight line. A thing to think of when lofting with an open loop is that the ellipses have to be created out of two loops. This means that the ellipses should be divided into two pieces. To create the transversal sealing straight lines are created to make the transversal sealing 5 mm width. Finally a shell loft is performed between the fluid end

line and the new created line. The longitudinal sealing is created by applying double package material thickness at the area where the longitudinal sealing is positioned. The skin modelling procedure continues as in section 7.1.2.

7.2 Element types

The size of the element is important for the accuracy of the solution. A too rough mesh gives an inaccurate solution and a too fine mesh brings a more accurate solution but at the sacrifice of a long solution time. The mesh density in the current FE-model has the size of 1.1 mm and the time increment is $1.5 \cdot 10^{-7}$ s. It is now possible to determine the solution time of this analysis according to (4.19). The mesh density will be examined further on in this thesis. To obtain a good mesh, different types of elements are used. The FE-model is mainly meshed with a structured mesh but close to the transversal sealings tetrahedron mesh are applied since the geometry is very complex in this area. Shell elements are used to mesh the skin since the package is very thin. There are different types of shell elements in ABAQUS/Explicit, for this case the $S4R$ and $S3R$ elements are used. The $S4R$ element has 4 nodes and the $S3R$ element has 3 nodes. These shell elements have conventional stress and displacement properties and a large-strain formulation [3]. They can be used in three dimensional dynamic analyses and allows mechanical loading. The shell elements also support reduced integration. This means that fewer Gauss points are used to calculate the stiffness but the mass matrix and loads are integrated exactly. The problem with using fewer Gauss points is the rigid-body motions. These can occur for other displacements than the real rigid-body motion. This depends on that fewer Gauss points can not describe the element in the same way as full integration. In solutions with full integrations the stiffness matrix is often too stiff while the reduced integration soften the stiffness. If the rigid-body motion is controlled the reduced integration may give a more accurate FE-model due to the stiffness matrix [11]. Another advantage with reduced integration is that the running times are shorter than with full integration. It should also be mentioned that full integration is not possible for $S4R$, $S3R$ and $C3D8R$ in ABAQUS/Explicit. When using reduced integrated elements it is necessary to be aware of that the hourglassing phenomena can occur.
The fluid part is modelled with solid elements. The fluid properties of the elements are received by defining the density and EOS, according to chapter 6.2. Appropriate solid elements for this analysis are the $C3D8R$ respectively $C3D4$ element. These are three dimensional solid elements with 8 nodes. The element structure in the FE-model can be seen in Figure 7.5.

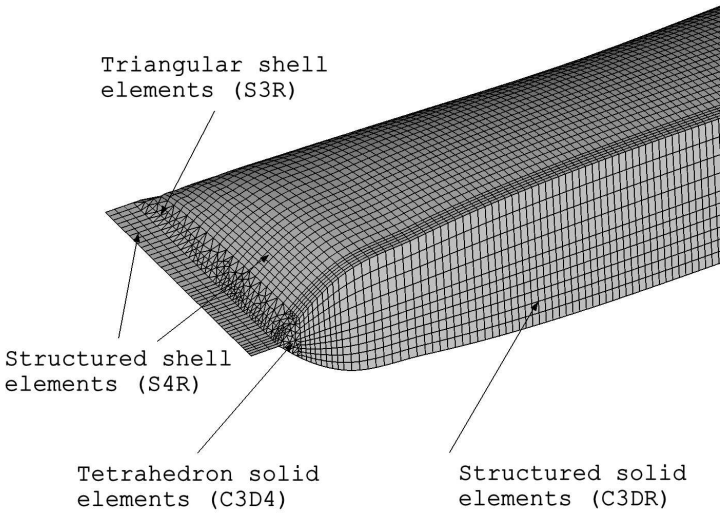

Figure 7.5: The element types in the FE-model.

The floor is modelled as an infinitely stiff part with infinite mass. Therefore the floor is only modelled with one element to reduce the computational effort. The element type that is used in the floor is the $R3D4$-element. This is a three dimensional rigid element with four nodes, the third dimension is established by a thickness of the element.

7.3 Assigning packaging material

The package contains both polymer and paperboard. The packaging material has higher strength properties in MD than in CD. This material behaviour is important to add in the FE-model. The material orientation is assigned in the FE-model by creating a local coordinate system in the package and every element gets an appropriate material orientation. A shell element definition has 1- and 2-direction in the plane and the 3-direction is always the shell normal. The material parameters were established in chapter 6.

7.4 Boundary conditions

To solve the dynamic event, boundary conditions have to be introduced in the FE-model. One of the most crucial conditions is the gravity but also the initial velocity and the impact point are important. Air resistance is ne-

glected in the analysis. To reduce the computational effort in the simulation, the package will always be dropped 1 mm above the floor. To be able to FE-simulate various heights the velocity of the package just before impact will be calculated. This is based on the law of energy conservation that determines the connection between the drop height and the position above the floor.

$$mgh_1 + \frac{mv_1^2}{2} = mgh_2 + \frac{mv_2^2}{2} \tag{7.1}$$

$$v_2 = \sqrt{2g(h_1 - h_2)} \tag{7.2}$$

The velocity calculated with 7.2 will be the initial velocity in the FE-simulation. The velocity and gravity should be applied to both the package and the fluid inside. The initial velocities and the corresponding kinetic energies that will be considered in these simulations are reported in table 7.1 In the FE-

Height [m]	0.3	0.8	1.3
Velocity [m/s]	2.4	4.0	5.1
Energy [J]	0.7	2.0	3.2

Table 7.1: Drop heights and corresponding initial velocities and energies.

simulation an impact point has to be established between the package and the floor. The impact point is where the package will hit the ground initially. In this thesis the package will be dropped in two orientations as described in chapter 8. The friction between the package and the floor is assumed to be negligible since the package falls perpendicular to the floor.

7.5 FE-simulations in ABAQUS/Explicit

In this section topics regarding solving analysis with the explicit method will be discussed, for example step increments, double precision, CPU-time and important information that is stored in the files produced by ABAQUS when submitting a job.
The total time in the FE-simulation should be adjusted to the problem to get an efficient simulation. This means that a long total time results in an unnecessary huge computational effort, long solution time and large result files, especially the *.odb-file. These problems can be reduced in following ways. As already mentioned the total time should be minimized to reduce the solution time. To reduce the solution time a higher number of CPU:s, Central Processing Unit, can be used for the explicit time integration method. This

is a very efficient method since the solution time can be decreased by 50 % using two CPU:s. Another way to decrease the size of the files is to optimize the step increment. In the step increment the user decides the frequency the solution stores data.
It is recommended to use the option double precision when submitting a job in ABAQUS/Explicit. Double precision means that more accurate numbers are used in the calculations, the floating point word lengths of 64 bits and then the noise will be reduced in the simulation [3].
When submitting a job in ABAQUS a number of files are produced and it is a bit difficult to find valuable information in them. Therefore a short overview will be made to bring forward the most utilized files. The most useful files are the *.inp, *.dat and *.sta files. Interesting information that can be found in the *.sta and *.dat files are summarized in table 7.2. The *.inp-file stores information from the CAE-module and is the file that is submitted to the solver. It is a good idea to use the *.inp-file for data check. That means to check if all data is correct applied, for example in this case the initial velocity or the time step.

CPU-time	*.sta	number of elements	*.dat
time increment	*.sta	element size	*.sta
total mass	*.sta	warnings	*.dat & *.sta
kinetic energy	*.sta	errors	*.dat & *.sta

Table 7.2: Valuable information stored in the *.sta and *.dat files.

7.6 Summary of the modelling procedure

Now it is time to summarize the modelling procedure to get a better overview of the FE-model. The reader is asked to consult appendix A for a schematic overview in ABAQUS/CAE. The scheme is a presentation of the various settings and parameters that are of importance. In this analysis SI units are used. At first we have a fluid part with a skin of shell elements at the surface that corresponds to the package geometry. The modelling procedure with skin was chosen since a better interaction was achieved between the package and the fluid. The package material model has orthotropic properties in both the elastic and plastic range. The orthotropic properties are assigned according to the material orientation in the package. The fluid is modelled with solid elements and receives its fluid properties by the equation of state, EOS. The components, longitudinal sealing and transversal sealings, are created in

the FE-model with some simplifications. The longitudinal sealing has double thickness of packaging material symbolizing the overlap but no strip. The transversal sealings are approximated to double package material thickness and triple in the region where the longitudinal and transversal sealing cross. Further the package is given an initial velocity and is dropped 1 mm above the floor to reduce the computational time. In this case it is also possible to decrease the computational time by performing the calculations on two CPU:s.

Chapter 8

Parameter variation and result

This chapter will cover the parameter variation of important settings in the FE-simulations and the results. The parameters that will be studied are variable drop heights, the orientation of the package when it hits the floor and material parameters. The package will be dropped from two orientations shown in Figure 8.1. The first orientation is a drop where the longitudinal sealing is parallel to the floor and will be called the horizontal fall. This will be the most common test position in the FE-simulations since this is the standard position in the experimental drop test. The second choice is to let the transversal sealing hit the floor first and this will be called the vertical fall. All the FE-simulations will be performed at the reference height 0.8 m except those where various heights will be tested.
When the package is drop tested it will hit the floor twice. The FE-simulations will only cover the first impact in order to reduce the solution time and the size of the files. The first impact is defined from the starting point until the entire package has left the floor. It is assumed that the critical stage for the package is during the first impact. If the package fractures it will probably happen during the first impact.
The package has an ideal sealing in the FE-model that means that the sealing will not burst. This depends on the modelling procedure where the transversal sealings are modelled as a straight lines and not with contact conditions. To model a crack mechanism a tensile failure condition could be applied but this is only possible for isotropic materials in ABAQUS.

8.1 Horizontal fall

The packages are FE-simulated from various heights. This is done to investigate if it is possible to detect differences in the FE-simulation. The drop

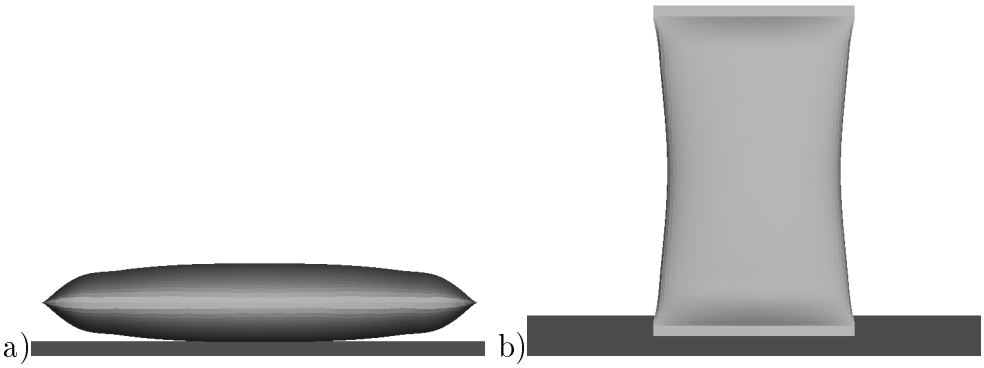

Figure 8.1: Two main orientations of the package in the FE-simulations, a)horizontal orientation and b) vertical orientation.

tests are performed from 0.3 m, 0.8 m and 1.3 m. These heights are chosen since they represent three different scenarios. The package can handle a drop from 0.3 m and this height represent the intact package behaviour while the 1.3 m drop corresponds to the damage package. A drop from 0.8 m is a reasonable height from which the package should stay intact. One way to study if the FE-simulation behaves correct is to control the impulse of the dropped package. This is performed by calculating the momentum before and after the impact.

$$I = \int_0^t F(t)dt = m(v_0 - v) \tag{8.1}$$

When performing drop tests it was observed that the package hits the floor in various ways, since the package rotates during the fall. To capture this phenomenon one package is rotated in the FE-simulation to hit the floor in an angled orientation. The orientation at impact will be estimated from a high-speed film.

8.1.1 Result

The deformation in the FE-simulation will mainly occur on the upside where the package dents as seen in Figure 8.2. Another deformation that is detected is a fold at the long sides of the package. When the package hits the floor the shock wave propagation can be seen on the underside. This is also reflected in high stress concentration on the impact side, in both tension and compression in the machine direction.

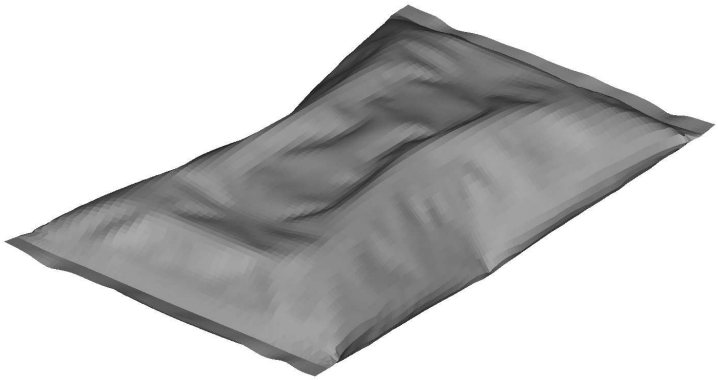

Figure 8.2: Deformation of a package dropped from 0.8 m at 4.5 ms.

Variable drop heights

The purpose to FE-simulate the three various heights was to detect differences. It is difficult to see different stress levels but it is possible to detect variation in the concentration areas in the machine direction. These can be seen in Figure 8.3. In the cross machine direction no differences can be distinguished and therefore will no picture of this behaviour be presented. Another interesting parameter to evaluate is the shear stresses since cracks with diagonal propagation have been detected in experimental drop tests. The shear stress in the plane direction is examined. For the shear stress concentrations, no variations can be noticed between the heights. The shear stress for the drop from 0.8 m is presented in Figure 8.4. The amount of the shear stresses can not be investigated further in this thesis since this material data has not been determined for this material at Tetra Pak. The area with shear stresses corresponds with the regions where the cracks appear, compare Figure 8.5.

One way to investigate when the impact occurs is to analyze the reaction forces in the floor. Various heights give different reaction forces in the floor. The reaction forces increases with the drop height as indicated in Figure 8.6. The graph also shows that the impact time last longer for low drop heights. Since the packages are dropped 1 mm above the floor with an initial velocity the package with the highest speed will hit the floor first. The reaction forces

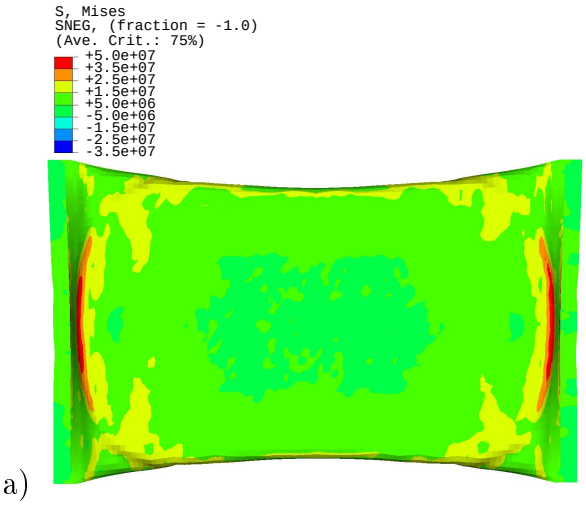

a)

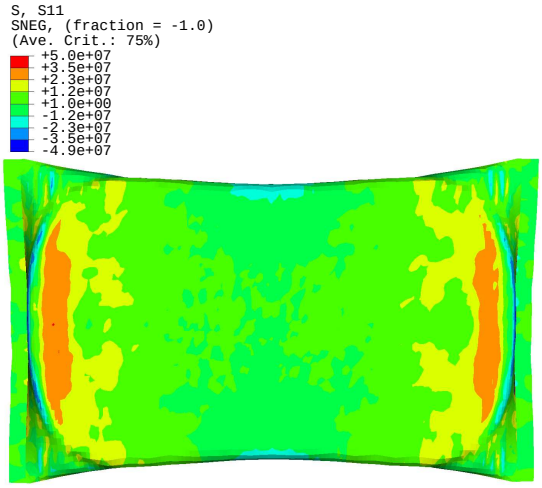

b)

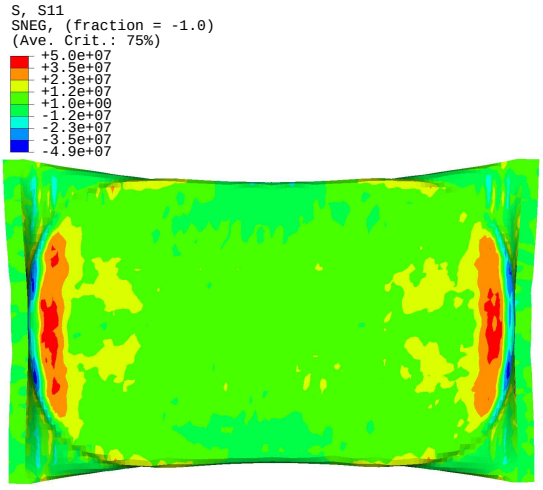

c)

Figure 8.3: Stress [Pa] in the machine direction -11 for the drop height a) 0.3 m, b) 0.8 m and c) 1.3 m from a underside view.

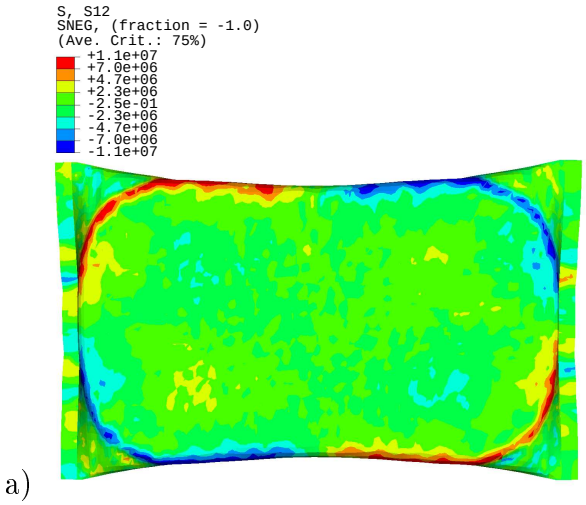

a) 2 ms

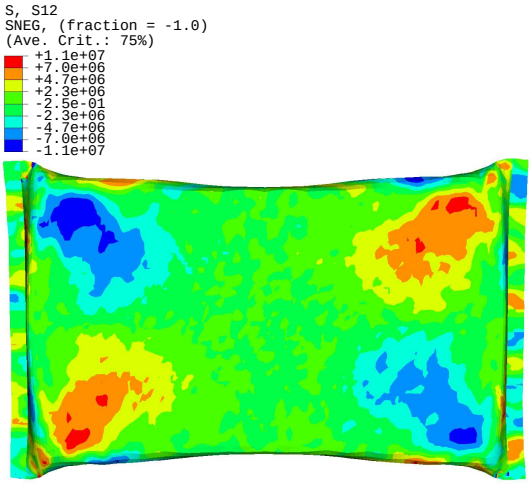

b) 2.5 ms

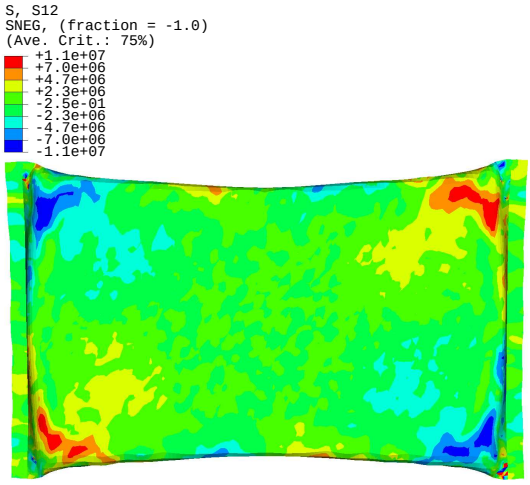

c) 3 ms

Figure 8.4: Shear stress propagation in MD-CD for the drop height 0.8 m from a underside view.

a) 

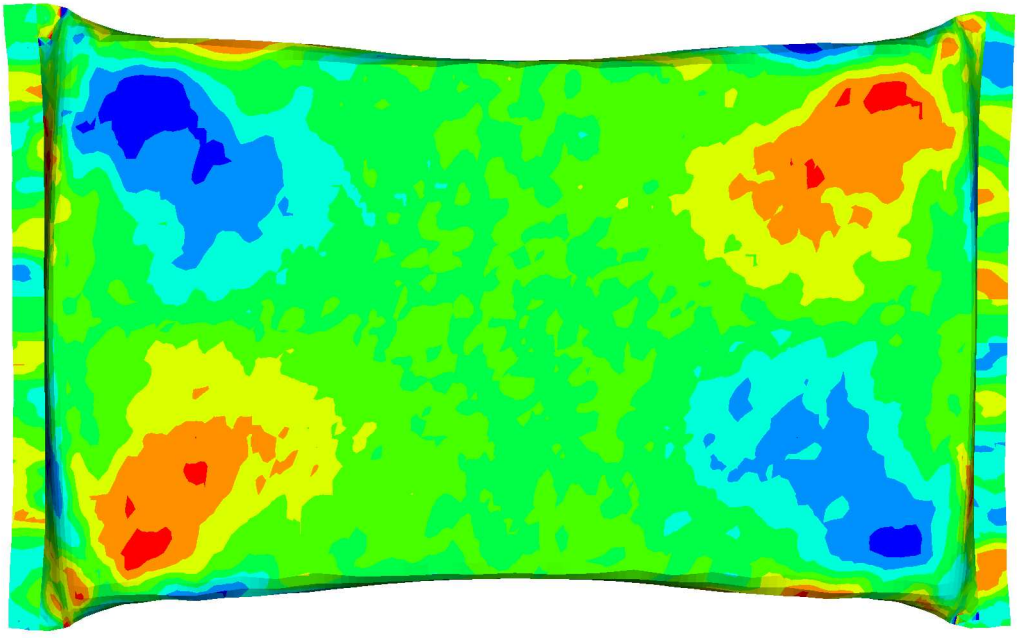

b)

Figure 8.5: a) Location of a material crack. b) Location of shear stress.

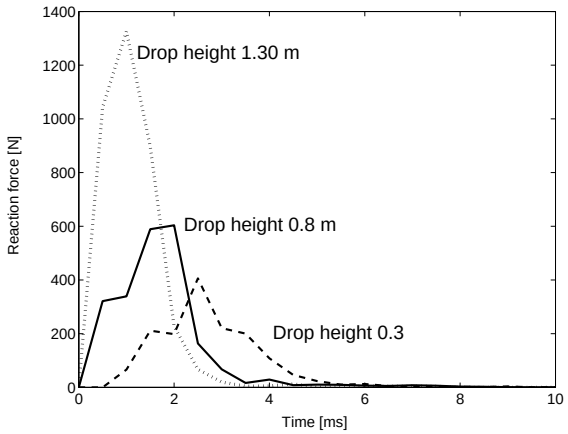

Figure 8.6: Reaction forces in the floor for various drop heights from horizontal falls.

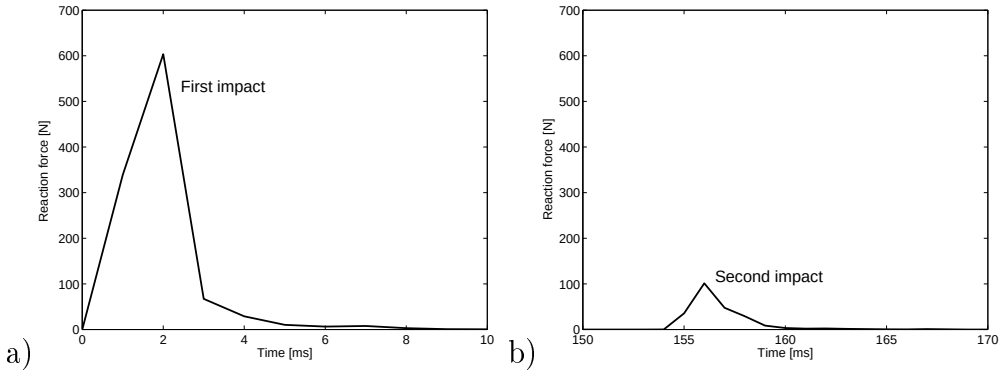

Figure 8.7: Reaction forces in the floor from a 0.8 m drop during a) first impact and b) second impact.

in Figure 8.6 are not linear with the drop heights since the drop height is not linear with the velocity. The areas under the graphs in Figure 8.6 represent the impulse that is defined in (8.1). The impulse is calculated by estimating the velocities in the momentum before and after impact. The result is found to be similar when comparing with the areas under the graphs. The appearance of the graphs in Figure 8.6 depends on that few time interval points have been saved in the FE-simulation. The amount of data points that are saved highly affects the size of the solution file. This is the reason that only 40 data points are saved. The package's first impact occurs after 2.0 ms for the drop that symbolize the height 0.8 m. The second impact occurs at 120 ms, presented in Figure 8.7, after that the package only has small movements.

Evaluation with high-speed films
The horizontal falls are compared with high-speed films. It is difficult to obtain a complete horizontal impact in the drop test setup, section 5.1 since the fork tilt when it is withdrawn and may cause the rotation of the package. Another reason to this behaviour is that the centre of gravity is displaced in the package during the fall. The problem to obtain a complete horizontal fall leads to that the impact time differ between the high-speed film and the simulated animation. A FE-simulation with an estimated impact orientation will be performed to simplify the evaluation procedure of the behaviour. This fall will be evaluated against a high-speed film in Appendix B. It is difficult to achieve an estimated angle that corresponds with the angle in the high-speed film. The problem is complicated by the rotation that often occurs in practical drop test. This is why the deformation does not occur in the same areas in the two cases. It is possible to see a tendency to similar behaviour between the FE-simulation and the high-speed film.

8.2 Vertical fall

The vertical fall is tested in the FE-simulation to observe if it is possible to capture the large deformations in the FE-simulation program, presented in chapter 3, that occur in this type of fall.

8.2.1 Result

When the package is dropped in a vertical orientation the water is gathered in the lower part of the package. This leads to large deformation in this region. This behaviour corresponds well with the high-speed film. The difference is that the package in the FE-simulation has larger deformations on the long sides. The comparison can be seen in Appendix B. The impact time in the high-speed film is estimated to 40 ms compared to the time in the FE-simulation that is 27 ms. It is difficult to establish the impact time in the high-speed film since the dissolution is not as good as in the FE-simulation films. This could be a reason that the impact time differs. Another source of errors could be that the air resistance is negligible in the FE-simulation. The reaction force for the vertical fall is much lower than for the horizontal as seen in Figure 8.8 but the impact last longer. This indicates on a more gentle impact for the vertical than the horizontal fall. The impulses in Figure 8.8 are theoretically the same. When calculating the areas in the graphs the

results are quite similar to each other.

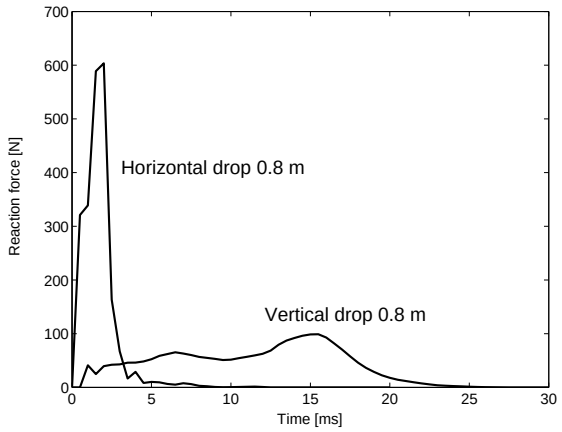

Figure 8.8: Reaction forces for the vertical and the horizontal fall.

8.3 Longitudinal sealing

A standard drop test is performed with the longitudinal sealing pointing upwards. One FE-simulation will be performed where the longitudinal sealing is placed downwards. Downwards means that the longitudinal sealing hits the floor first. This is done to evaluate if the packages react differently during impact.

8.3.1 Result

The FE-simulation procedure behaves in the same way whether the longitudinal sealing is placed upwards or downwards. The difference that could be detected was larger stress concentrations around the longitudinal sealing in the machine direction when the sealing was placed downwards. The stress concentrations are normally distributed over a larger area in the standard drop orientation. No differences could be detected in the high-speed films between the longitudinal sealing positioned upwards or downwards. It was difficult to compare them against the FE-simulation since the filmed package orientations were not perpendicular to the floor.

8.4 Material

To investigate the material dependency a thinner thickness was tested in the FE-simulation. The thickness was reduced by 20%.

8.4.1 Result

No differences were found when reducing the material thickness. The stresses and shear stresses were at the same level as before. The material properties out of the plane cannot be controlled since shell elements are used to create the packaging material.

8.5 Mesh density

In the explicit solution method the energy levels are controlled to establish the correctness in the discretization of the FE-simulation model. If the energy levels are acceptable a mesh density with fewer elements can be tested to achieve a shorter solution time. A mesh containing a larger amount of elements can also be tested to investigate if the deformation obtains a smother appearance.

8.5.1 Result

At first a mesh containing less elements than the existing mesh was tested but this mesh resulted in unstable energy levels according to Figure 8.9. The internal energy increased which is an indication for a bad mesh. Then a mesh containing a larger amount of elements was tested. This resulted in the same energy levels as the existing mesh in Figure 8.9. The mesh with larger amount of elements had a 25% longer solution time than the existing mesh. Even though a smother appearance is obtained the cost of a longer solution time is considered to be to high.
The interesting energies to investigate are plotted in Figure 8.9 and Figure 8.10. The total energy is supposed to be constant in the solution and should not vary more than 1% [3]. The total energy level in Figure 8.9 is constant. The initial level of the kinetic energy can be controlled in this FE-simulation since this can be established from the energy of conservation law, Table 7.1. The kinetic energy will then decrease and the internal energy will increase. The internal energy consists of the strain energy and plastic dissipation. The strain energy will increase during the impact and will then turn back since this only measures elastic deformation. The plastic dissipation will also

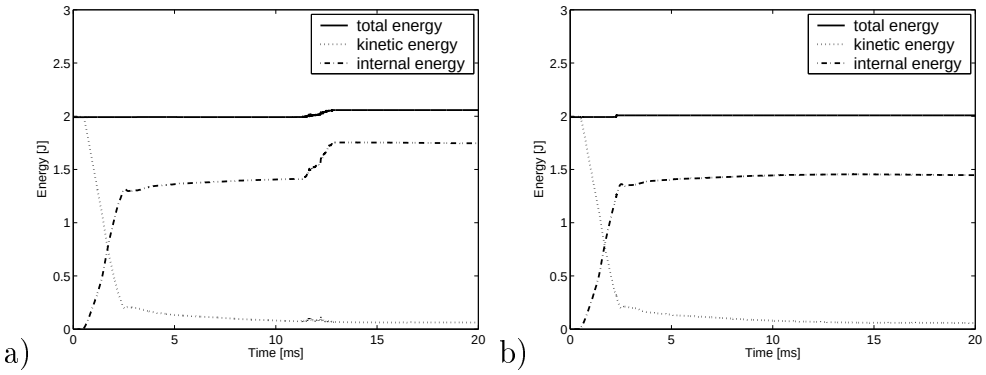

Figure 8.9: a) Bad energy plot for the mesh containing less elements. b) Energy plot from the reference mesh.

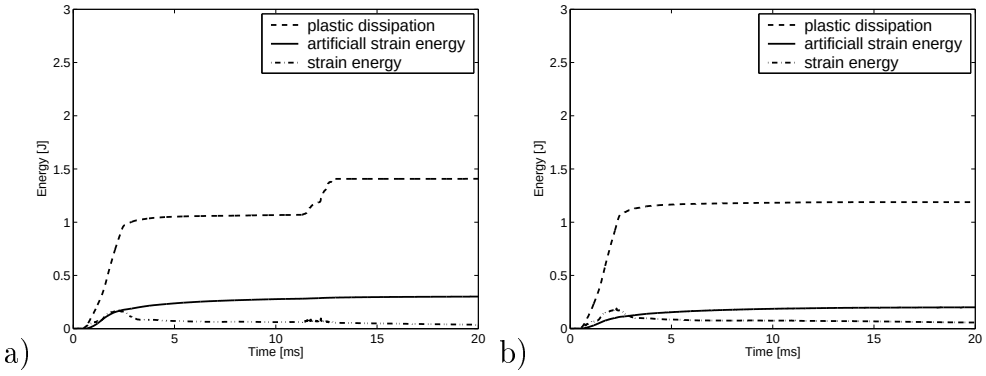

Figure 8.10: a) Bad energy plot for the mesh containing less elements. b) Energy plot from the reference mesh.

increase during the impact but will then be stabilized since it measures a permanent deformation. The artificial energy should be kept much smaller than the internal energy. In this case the artificial energy level is checked by enhanced hourglass control. Therefore the artificial energy level is assumed to be corrected [3].

Chapter 9

Discussion

The FE-model with skin was selected among three different modelling techniques. This FE-model was chosen since it captures the interaction between the packaging material and liquid the best. In the FE-simulations several parameters have been studied. The package has been simulated in horizontal and vertical drops. The package in the FE-simulations behaved quite similar to the reality. This was concluded after analyzing the high-speed films and conducting practical tests. The phenomena that occur during an impact is that the upside of the package can deform while the impact side have no ability to deform that leads to high stresses on this side. No differences were observed in the deformation behaviour when the high-speed films of the three drop-heights were compared. Neither could a difference be detected in the deformation behaviour for the various heights in FE-simulation model. When comparing the high-speed films with the FE-simulations similarities in the deformation behaviour were observed, even thou an estimated orientation is FE-simulated it is hard to fully capture the deformation behaviour. The package cannot burst since no fracture conditions are applied in the FE-model. In the evaluation process stress concentrations in the MD-CD plane was controlled in the packaging material. The package is modelled with shell elements and therefore the stresses out of plane direction cannot be examined. It is unfortunately not possible to evaluate the sealing areas since they are modelled as perfect sealings. The stress concentrations that occur around the transversal sealings cannot be evaluated since the cause of the stresses depends on geometry inaccuracy.
In this thesis the dynamic pendulum was tested to investigate if a strength parameter in the transversal sealing could be obtained. Unfortunately, no useful result was obtained. An idea is to use a pendulum with a smaller mass to investigate if a more precise result can be achieved. If this idea will be tested the energy level in the pendulum should be a bit higher than the

energy absorption in the samples. Hopefully this adjustment will result in more accurate energy levels. If not so, the test method might not be suitable to measure the strength in the sealing.

9.1 Conclusion

The final modelling technique is simple and easy to use. The benefit with this strategy is that it is easy to update the geometry in the FE-model. The geometry of the package can be controlled. For the aseptic pouch the circumference, volume and mass can be verified against the real package. It is also possibly to apply this technique on similar packages. The difficulties were to capture the large deformation of a soft package and the interaction between the liquid and the package. The behaviour of the dropped packages in the FE-simulations corresponds well compared to the high-speed films.
The FE-simulations show that high stress concentrations occur on the underside of the package. This seems to correspond well to the experimental drop tests since the material often fractures on this side. An observation is that the cracks in the material often propagates diagonal from the corners. The shear stresses in MD-CD indicate on stress concentrations in the exposed areas. This result could be further investigated to establish if such a correlation exists. Differences in the stress concentration areas were detected in the machine direction between the heights. This could be an interesting parameter to evaluate further since the affected areas could help to determine if a package can resist a drop.
The reaction forces in the vertical fall are much smaller than for the horizontal. This is due to a larger amount of water that hits the floor at the same time in the horizontal fall. In the vertical fall the package has a better capability to deform. The impact will also last for a longer time but the total impulse will be the same. The conclusion is that the vertical fall has a more gentle impact than the horizontal fall. The horizontal fall can therefore be defined as the most critical impact orientation. This behaviour corresponds well with the knowledge in project at Tetra Pak.
The measurements obtained in the dynamic pendulum test did not indicate on any differences between the tested samples. One conclusion that could be drawn is that the pendulum probably is too heavy.
Finally, the main purpose of this thesis is achieved since it has been shown that it is possible to FE-simulate the dynamic event of a soft package drop test. Unfortunately no specific parameter that can predict the critical drop height has been detected.

9.2 Further Work

To obtain better results several things can be improved in the FE-model. Specific areas that need to be improved are the sealings and the material description. To be able to evaluate the transversal sealings the present sealings need to be replaced by a contact definition. It would therefore be desirable to have a measurement of the strength in the sealing to implement in the contact definition.
The material description can be improved by assigning the properties by the lamina command in ABAQUS. Each layer can be defined with the lamina command. This will allow the material to have different bending properties in tension and compression. If it is desired to study the delamination between the layers a model of the sealing should be created and implemented with 3DM [12]. The 3DM-model considers both a continuum model and an interface model where the interface model determines the delamination.
To investigate if there is a connection between the cracks and the shear stresses experimental test can be used to find this parameter. If the materials show different strengths in the shear test this could explain why some materials cracks easier.
The drop test equipment can be improved by putting a high-speed scale on the floor to measure the reaction forces during the impact. This would bring a measurement to evaluate in the drop test method. The reaction forces could be compared with the ones calculated in the simulation.

Bibliography

[1] Tetra Pak Marketing Services AB, *Promotional Material*,Lund, Sweden.

[2] T. Belytschko, Wing Kam Liu & Brian Moran *Nonlinear Finite Elements for Continua and Structures*, Wiley 2001.

[3] ABAQUS *documentation, Version 6.5*

[4] O.C. Zienkiewicz & R.L. Taylor *The Finite Element Method*, Volume II. Butterworth Heinemann, Fith Edition, 2000.

[5] N. S Ottosen and M. Ristinmaa *The Mechanics of Constitutive Modelling*, Volume I-II, Division of Solid Mechanics, Lund University, 1999.

[6] A. Harrysson, M. Harrysson & M. Ristinmaa *Current Models for Paper and Paperboard*, Division of Solid Mechanics, Lund University, 2003.

[7] C. Führer & A. Schroll *Numerical Analysis - An Introduction*, 6th Edition, Lund University, 2004.

[8] K.Persson *Material model for paper - experimental and theoretical aspects*, Division of Structural Mechanics, Lund University, 1991.

[9] O.C. Zienkiewicz & R.L. Taylor *The Finite Element Method*, Volume III. Butterworth Heinemann, Fith Edition, 2000.

[10] http://hyperphysics.phy-astr.gsu.edu/hbase/sound/souspe2.html#c1, *HyperPhysics* Georgia State University

[11] N. S Ottosen & H. Petersson *Introduction to the Finite Element Method* Prentice Hall Europe, 1992.

[12] O. Elison & L. Hansson *Evaluating the 3DM model - an experimental and finite element study*, Division of Solid Mechanics, Lund University, 2005.

Appendix A

Package modelled in ABAQUS

A mind map was created to get an overview of the parameters used in the FE-simulation model. The map is based on the module setup in ABAQUS/Explicit. This mind map is created to increase the understanding for the modelling technique. The parameter variation that were discussed in chapter 8 are marked in the mind map.

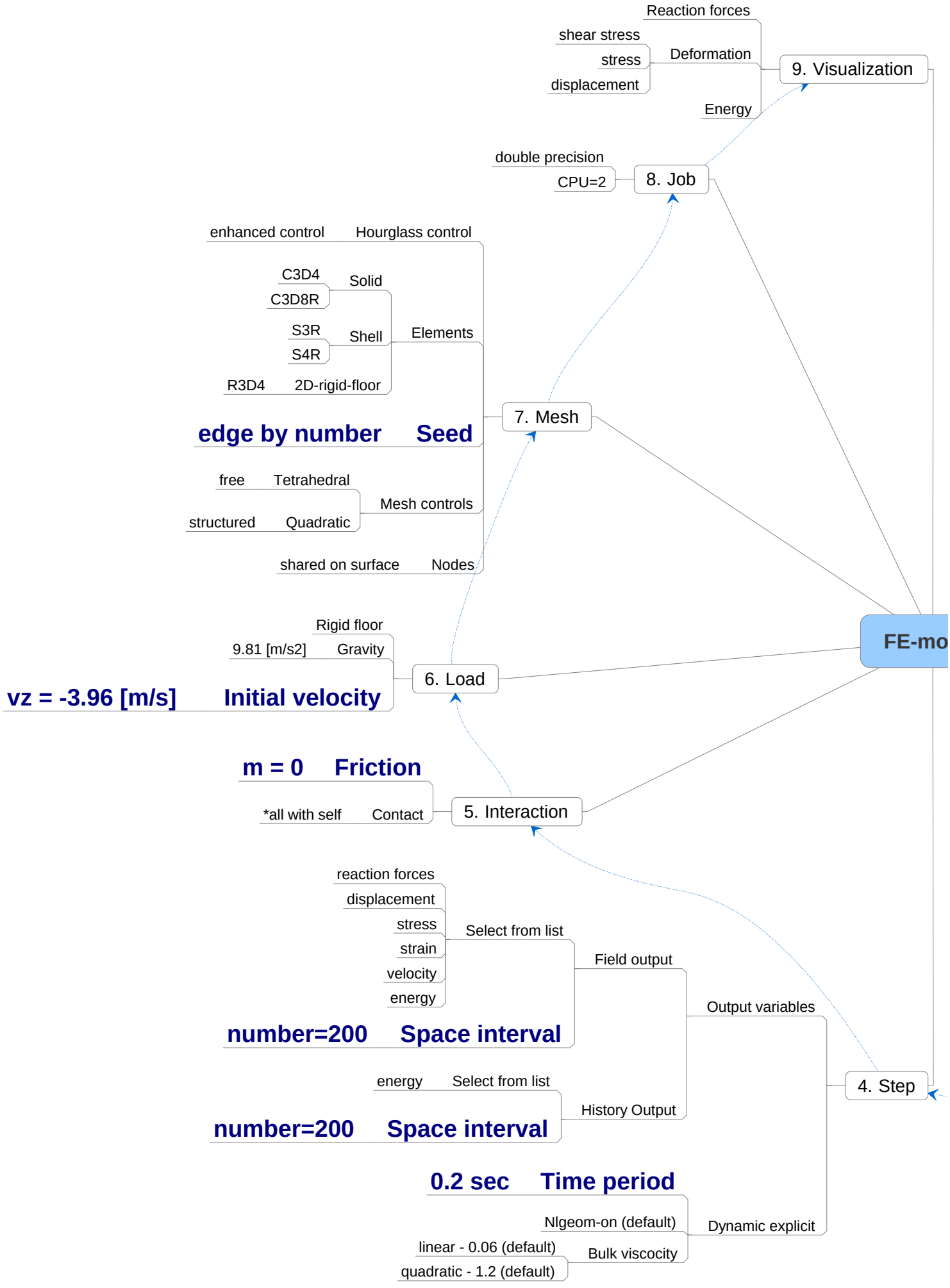
FE-mo
9. Visualization
Reaction forces
shear stress
stress
displacement
Deformation
Energy
8. Job
double precision
CPU=2
7. Mesh
enhanced control
Hourglass control
C3D4
C3D8R
Solid
S3R
S4R
Shell
Elements
R3D4
2D-rigid-floor
edge by number
Seed
free
Tetrahedral
structured
Quadratic
Mesh controls
shared on surface
Nodes
6. Load
Rigid floor
9.81 [m/s2]
Gravity
vz = -3.96 [m/s]
Initial velocity
m = 0
Friction
*all with self
Contact
5. Interaction
reaction forces
displacement
stress
strain
velocity
energy
Select from list
Field output
number=200
Space interval
energy
Select from list
History Output
number=200
Space interval
Output variables
4. Step
0.2 sec
Time period
Nlgeom-on (default)
linear - 0.06 (default)
quadratic - 1.2 (default)
Bulk viscocity
Dynamic explicit

(SI-units)

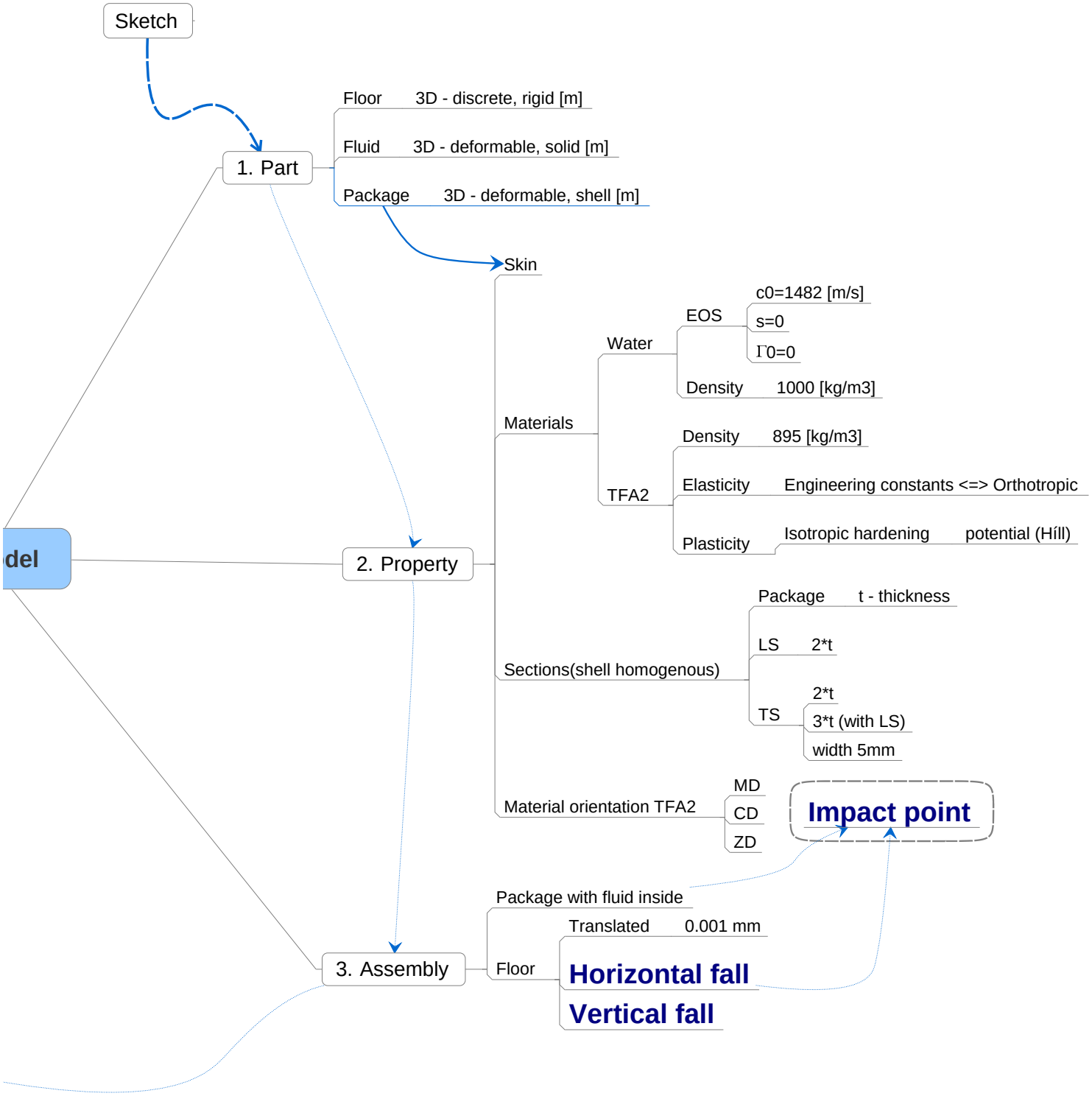
Sketch
1. Part
Floor 3D - discrete, rigid [m]
Fluid 3D - deformable, solid [m]
Package 3D - deformable, shell [m]
Skin
Materials
Water
EOS
c0=1482 [m/s]
s=0
Γ0=0
Density 1000 [kg/m3]
TFA2
Density 895 [kg/m3]
Elasticity Engineering constants <=> Orthotropic
Plasticity Isotropic hardening potential (Híll)
del
2. Property
Sections(shell homogenous)
Package t - thickness
LS 2*t
TS
2*t
3*t (with LS)
width 5mm
Material orientation TFA2
MD
CD
ZD
Impact point
Package with fluid inside
Translated 0.001 mm
3. Assembly
Floor
Horizontal fall
Vertical fall

Appendix B

Comparing FE-simulations with high-speed film

A comparison between the FE-simulated drops and the high-speed films will be shown in three picture sequence. These pictures are shown to give the reader an opportunity to observe the resemblance in the behaviour. The first set of pictures describes the similarities in a horizontal fall from a side view in Figure B.1. The high-speed film captures the real behaviour the package experience during a fall from rest. The package in the simulation is placed in a similar angle to the floor to obtain a better agreement to the reality. The next picture series shows the same event but is filmed in an angle from above in figure B.2. The last picture sequence presents a vertical drop position of the package in Figure B.3. All the drops in the pictures are performed from 0.8 m.

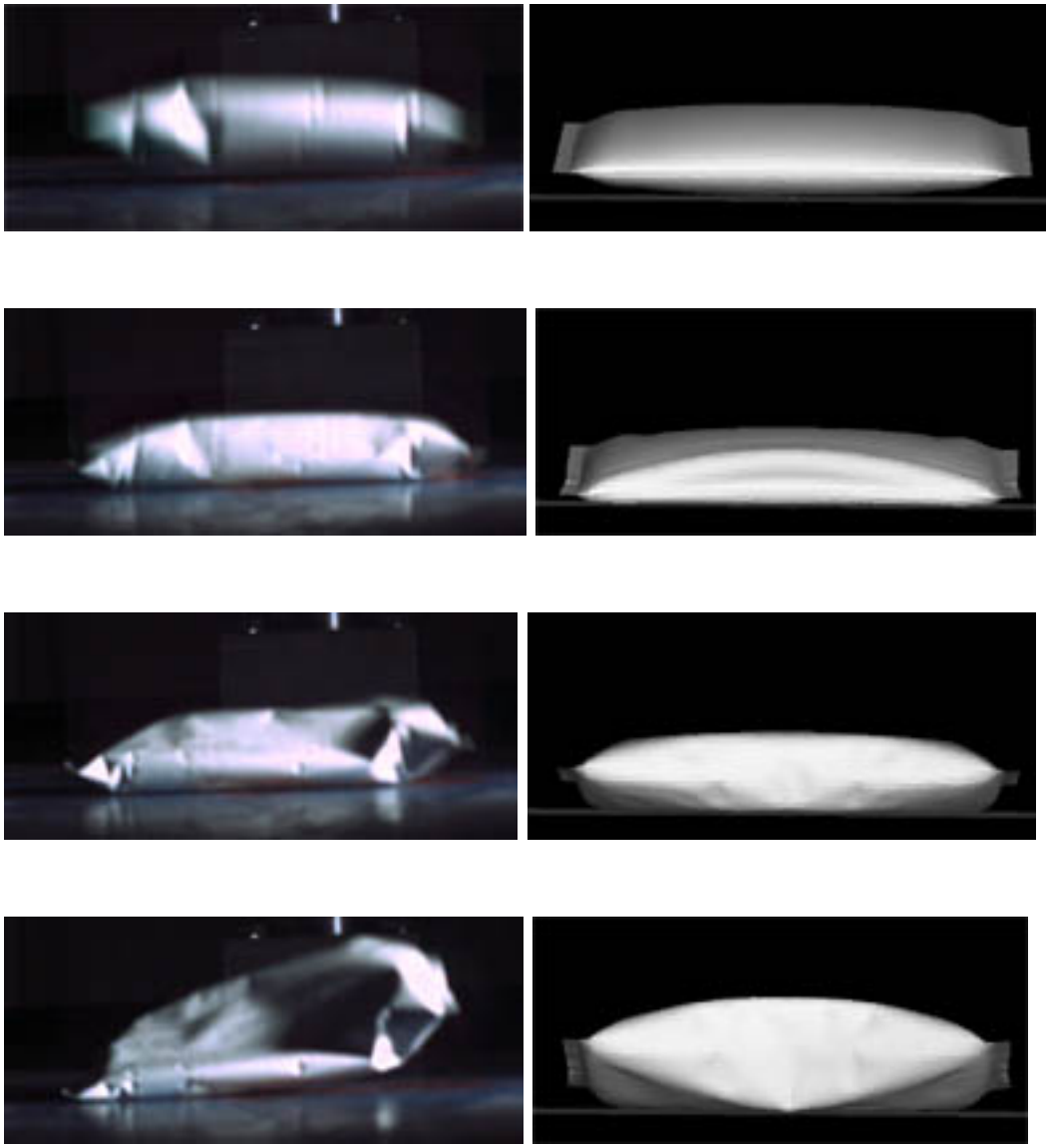

Figure B.1: Comparing horizontal falls in a side view.

Figure B.2: Comparing horizontal falls in a view from above.

Figure B.3: Comparing vertical falls in a side view.

Appendix C

ABAQUS/Explicit input-file

```
*Heading
** Job name: DropSoftPackage Model name: nominell_model
*Preprint, echo=NO, model=NO, history=NO, contact=NO
**-----------------------------------------
**
***            PART-FLOOR
**-----------------------------------------
**
*Part, name=Floor
*Node
      1,         -0.5,         -0.5,           0.
      2,          0.5,         -0.5,           0.
      3,         -0.5,          0.5,           0.
      4,          0.5,          0.5,           0.
*Element, type=R3D4
1, 1, 2, 4, 3
*Node
      5,           0.,           0.,           0.
*Nset, nset=Floor-RefPt_, internal
5,
*Elset, elset=Floor
 1,
*End Part
**-----------------------------------------
**
***            PART-FLUID
**-----------------------------------------
**
*Part, name=Fluid_content
*Node
      1,           0.,           0., -0.0724999979
      2,           0.,           0., -0.0764999986
      .
      .
      .
  62669, -0.0414670259, 0.00237717107, -0.066967614
  62670, -0.0413612947, 0.00255432609, -0.0659830123
**
*Element, type=C3D4
      1, 28283,  5061, 28284, 28285
      2, 28283,  5123, 28285, 28286
      .
      .
      .
   8809, 7177, 7178,  690,  689
   8810, 7178, 1369,   41,  690
  62260,  101, 1521, 7633, 1528
  62261, 1521, 1522, 7634, 7633
      .
      .
      .
 74236, 10505, 10504,  2296,  2295
 74237,  2304, 10505,  2295,   164
**
*Element, type=C3D8R
   8811,     4,  1058,  7179,  1376,   328,  6816, 28615,  7191
   8812,  1058,  1057,  7180,  7179,  6816,  6817, 28616, 28615
      .
      .
      .
  62258, 62609, 62607, 62567, 62568, 28281, 28282, 28260, 28259
  62259, 62607,  9683,  9680, 62567, 28282,  2069,  2068, 28260
```

```
*Element, type=S4R
   8271,   73, 1174, 6843, 1196
   8272, 1174, 1175, 6844, 6843
      .
      .
      .
  62669, -0.0414670259, 0.00237717107, -0.066967614
  62670, -0.0413612947, 0.00255432609, -0.0659830123
**
*Element, type=S3R
74238, 6695, 6696, 1029
74239, 1049, 6694, 6697
      .
      .
      .
76808, 5095, 5112, 5114
76809,  355, 5107, 5114
**
*Nset, nset=TS
    3,    7 . . .
*Nset, nset=LSTS
    2,    3 . . .
*Nset, nset=LS
    59,  60 . . .
*Nset, nset=Skin_Package
    2,    3 . . .
**
** Region: (Water:Fluid_contetnt), (Controls:EC-1)
** Section: Water
*Solid Section, elset=fluid, controls=EC-1, material=Vatten
1.,
*Orientation, name=Ori-2
0.,           0.,           1.,           1.,           0.,           0.3,       0.
**
** Region: (Skin_Package:Skin_Package), (Controls:EC-1), (Material Orientation:Package)
*Elset, elset=Skin_Package, internal, generate
 63390,  74237,      1
** Section: Skin_Package
*Shell Section, elset=Skin_Package, orientation=Ori-1, controls=EC-1, material=Papper
0.000122, 5
*Orientation, name=Ori-1
0.,           0.,           1.,           1.,           0.,           0.3,       0.
**
** Region: (TS:TS), (Controls:EC-1), (Material Orientation:TS)
** Section: TS
*Shell Section, elset=TS, orientation=Ori-1, controls=EC-1, material=Papper
0.000244, 5
*Orientation, name=Ori-1
0.,           0.,           1.,           1.,           0.,           0.3,       0.
**
** Region: (LS_skin:LS_skin), (Controls:EC-1), (Material Orientation:LS)
** Section: LS_skin
*Shell Section, elset=_PickedSurf467, orientation=Ori-1, controls=EC-1, material=Papper
0.000244, 5
*Orientation, name=Ori-1
0.,           0.,           1.,           1.,           0.,           0.3,       0.
**
** Region: (LSTS:LSTS), (Controls:EC-1), (Material Orientation:LSTS)
** Section: LSTS
*Shell Section, elset=LSTS, orientation=Ori-2, controls=EC-1, material=Papper
0.000366, 5
*End Part
```

```
**-----------------------------------------
**
***                 ASSEMBLY
**-----------------------------------------
*Assembly, name=Assembly
**
*Instance, name=Fluid_content-1, part=Fluid_content
 3.49080188664863e-05, -0.0987023837026073, 0.0248711773551866
*End Instance
**
*Instance, name=Floor-1, part=Floor
 3.49080188526952e-05, -0.114702383702607, 0.0248711773551866
 3.49080188526952e-05, -0.114702383702607, 0.0248711773551866,
 1.00003490801885, -0.114702383702607, 0.0248711773551866, 89.9999990194245
*End Instance
**
*End Assembly
**-----------------------------------------
**
***              ELEMENT CONTROLS
**-----------------------------------------
**
*Section Controls, name=EC-1, hourglass=ENHANCED
1., 1., 1.
**-----------------------------------------
**
***                 MATERIALS
**-----------------------------------------
**
*Material, name=Papper
*Density
895.,
*Elastic, type=ENGINEERING CONSTANTS
 3.5e+09,  1.7e+09, 1.75e+07,     0.37,       0.,       0., 9.43e+08,  6.4e+07
  4.8e+07,
*Plastic
 1.7181e+07,     0.
    2.4e+07,  0.001
    2.7e+07,  0.002
    3.3e+07,  0.004
    3.7e+07, 0.0063
      4e+07,  0.008
    4.3e+07,   0.01
    4.7e+07,  0.012
      5e+07,  0.015
*Potential
1.,  0.5, 0.45,  0.4, 0.25, 0.15
*Material, name=Vatten
*Density
1000.,
*Eos, type=USUP
1482.,0.,0.
**-----------------------------------------
**
***             INTERACTION PROPERTIES
**-----------------------------------------
**
*Surface Interaction, name=fric
*Friction
0.,
**
** Interaction: Int-1
```

```
*Contact, op=NEW
*Contact Inclusions, ALL ELEMENT BASED
*Contact property assignment
 ,  , fric
**--------------------------------------------
**
***            BOUNDARY CONDITIONS
**--------------------------------------------
**
** Name: Rigid_floor Type: Symmetry/Antisymmetry/Encastre
*Boundary
_PickedSet109, ENCASTRE
**
***FIELDS
**
** Name: DropVel   Type: Velocity
*Initial Conditions, type=VELOCITY
Fluid_content-1.Fluid_contetnt, 1, 0.
Fluid_content-1.Fluid_contetnt, 2, -3.96
Fluid_content-1.Fluid_contetnt, 3, 0.
** Name: Package_Vel   Type: Velocity
*Initial Conditions, type=VELOCITY
Fluid_content-1.Skin_Package, 1, 0.
Fluid_content-1.Skin_Package, 2, -3.96
Fluid_content-1.Skin_Package, 3, 0.
** Name: TSVel   Type: Velocity
*Initial Conditions, type=VELOCITY
Fluid_content-1.TS, 1, 0.
Fluid_content-1.TS, 2, -3.96
Fluid_content-1.TS, 3, 0.
** Name: LS_vel   Type: Velocity
*Initial Conditions, type=VELOCITY
Fluid_content-1.LS, 1, 0.
Fluid_content-1.LS, 2, -3.96
Fluid_content-1.LS, 3, 0.
** Name: LSTS   Type: Velocity
*Initial Conditions, type=VELOCITY
Fluid_content-1.LSTS, 1, 0.
Fluid_content-1.LSTS, 2, -3.96
Fluid_content-1.LSTS, 3, 0.
**
***LOADS
**
** Name: gravity   Type: Gravity
*Dload
, GRAV, 9.81, 0., -1., 0.
**
**--------------------------------------------
**
***                   STEP
**--------------------------------------------
*Step, name=Step-1
*Dynamic, Explicit
, 0.02
*Bulk Viscosity
0.06, 1.2
**
**
*** FIELD OUTPUT: F-Output-1
**
*Output, field, number intervals=40
*Node Output
```

```
A, PCAV, RF, U, V
*Element Output, directions=YES
ELEDEN, ELEN, ENER, LE, PE, PEEQ, S
*Contact Output
CSTRESS, PPRESS
**
***HISTORY OUTPUT: H-Output-1
**
*Output, history, variable=PRESELECT, frequency=40
*End Step
```